Journal of Visualized Experiments

Fabrication of high contrast gratings for the spectrum splitting dispersive element in a concentrated photovoltaic system

--Manuscript Draft--

Manuscript Number:	JoVE52913R2
Full Title:	Fabrication of high contrast gratings for the spectrum splitting dispersive element in a concentrated photovoltaic system
Article Type:	Methods Article - JoVE Produced Video
Keywords:	Parallel spectrum splitting; dispersive element; high contrast grating; concentrated photovoltaic system; nanoimprint lithography; reactive ion etching
Manuscript Classifications:	7.1.60.249.730: Solar System; 93.33.44: lithography (circuit fabrication); 93.33.68: semiconductor devices; 93.37.49: materials fabrication; 97.74.31: optoelectronics (optics)
Corresponding Author:	Wei Wu University of Southern California Los Angeles, California UNITED STATES
Corresponding Author Secondary Information:	
Corresponding Author E-Mail:	wu.w@usc.edu
Corresponding Author's Institution:	University of Southern California
Corresponding Author's Secondary Institution:	
First Author:	Yuhan Yao, Ph.D.
First Author Secondary Information:	
Other Authors:	Yuhan Yao, Ph.D.
	He Liu
Order of Authors Secondary Information:	
Abstract:	High contrast gratings are designed and fabricated and its application is proposed in a parallel spectrum splitting dispersive element that can improve the solar conversion efficiency of a concentrated photovoltaic system. The proposed system will also lower the solar cell cost in the concentrated photovoltaic system by replacing the expensive tandem solar cells with the cost-effective single junction solar cells. The structures and the parameters of high contrast gratings for the dispersive elements were numerically optimized. The large-area fabrication of high contrast gratings was experimentally demonstrated using nanoimprint lithography and dry etching. The quality of grating material and the performance of the fabricated device were both experimentally characterized. By analyzing the measurement results, the possible side effects from the fabrication processes are discussed and several methods that have the potential to improve the fabrication processes are proposed, which can help to increase the optical efficiency of the fabricated devices.
Author Comments:	Dear Dr. Nam Nguyen, Many thanks for your letter of Jan. 29th 2015, with the editor's and reviewers' comments. We have carefully reviewed all their remarks and took them all into account. We believe that the amended manuscript is suitable for publication in JoVE. Given the urgency and timeliness nature of JoVE, we would appreciate to have your final decision at your earliest convenience. In addition, we provide below detailed responses to address those comments. Please let me know if you have any further comments. Sincerely yours,

	Yuhan Yao, He Liu and Wei Wu Department of Electrical Engineering, University of Southern California
Additional Information:	
Question	**Response**
If this article needs to be "in-press" by a certain date to satisfy grant requirements, please indicate the date below and explain in your cover letter.	
If this article needs to be filmed by a certain date to due to author/equipment/lab availability, please indicate the date below and explain in your cover letter.	

Dear Dr. Nam Nguyen,

Many thanks for your letter of Jan. 29th 2015, with the editor's and reviewers' comments. We have carefully reviewed all their remarks and took them all into account. We believe that the amended manuscript is suitable for publication in JoVE. Given the urgency and timeliness nature of JoVE, we would appreciate to have your final decision at your earliest convenience.

In addition, we provide below detailed responses to address those comments.

Please let me know if you have any further comments.

Sincerely yours,

Yuhan Yao, He Liu and Wei Wu
Department of Electrical Engineering, University of Southern California

Editorial comments:

1. Please take this opportunity to thoroughly proofread the manuscript to ensure that there are no spelling or grammar issues. The JoVE editor will not copy-edit your manuscript and any errors in the submitted revision may be present in the published version.
Please watch for missing periods at the end of sentences. Also, there are numerous missing articles as well: a, an, the, of, etc.

We have proofread the manuscript for spelling or grammar errors.

2. For volumes of the resist used, please define a "drop".

20 drops = 1 mL. We have added the definition to the protocol.

3. 1.1.6 / 1.2.4 - What pressure must the desiccator be pumped down to?

-30 inHg. We have added the definition to the corresponding steps in the protocol.

Reviewers' Comments:

Review #1:

1. In the protocol, deposition of TiO2 was not included. Since this is the key material for the device to be fabricated, a procedure of depositing this material should also be included in the protocol.

We have added the protocol of TiO_2 deposition to the protocol.

2. In real application, sunlight is focused on the dispersive element within a certain angle. What is reflectance of the device for sunlight slightly off from the normal incidence direction?

We added the following discussion to the paper. Due to its high index contrast between the grating and substrate, the high contrast grating has good angle independence. Unlike diffraction gratings, high contrast grating has similar reflectance when the incidence angle is less than 15°.

3. The fabricated device achieves a peak reflectance of about 60%. Since a significant amount of light is not reflected by this device, could the authors comment its implication on the overall efficiency of the concentrated photovoltaic device?

Generally speaking, the overall efficiency is the product of the optical efficiency and the solar cell conversion efficiency. Since the peak is about 60%, the overall efficiency will be 40% lower than expected value (40% for four-junction spectrum splitting). In order to achieve a higher overall efficiency, the fabrication process should be further optimized to increase the peak reflectance, which has been discussed in our paper.

Reviewer #2:

In the introduction, the authors stated that the designed dispersive element can be applied in reflective CPV system without prior discussion about the objective of the paper or any brief description for the proposed method. Then they describe the detailed steps. It would be informative for the reader to include a few lines in the introduction about the objective of the work and how the dispersive element will be designed and fabricated before stating the steps in bullets.

Thank you for your comments. We have added more background information at the beginbing of the introduction.

Reviewer #3:

1. Specifically what can be adjusted in the dry etching recipes that would give a better etching profile?

We have added the following discussion in the paper. A better etching profile can be achieved by adjusting the combination of gases (C_4F_8, SF_6 and O_2) to balance the etching and re-deposition process for a straighter side wall.

2. The roughness from the nano-imprint and lift-off process is inherent. What specifically can be done to improve this?

You are absolutely correct. Since nanoimprint is a sub-10nm fabrication technology, the roughness from the master mold will be inherited. To reduce the roughness, we should make a master mold with smoother edges. Various smoothing technologies have been reported. For example, smooth edge can be achieved by thermal process* or chemical anisotropic etching (e.g. KOH to etch silicon).

**Yu, Zhaoning, et al. "Fabrication of nanoscale gratings with reduced line edge roughness using nanoimprint lithography." Journal of Vacuum Science & Technology B 21.5 (2003): 2089-2092.*

TITLE:

Fabrication of high contrast gratings for the spectrum splitting dispersive element in a concentrated photovoltaic system

AUTHORS:
Yao, Yuhan
Department of Electrical Engineering
University of Sothern California
Los Angeles, CA
yuhanyao@usc.edu

Liu, He
Department of Electrical Engineering
University of Sothern California
Los Angeles, CA
heliu@usc.edu

Wu, Wei
Department of Electrical Engineering
University of Sothern California
Los Angeles, CA
Wu.w@usc.edu

CORRESPONDING AUTHOR:
Wu, Wei

KEYWORDS:
Parallel spectrum splitting, dispersive element, high contrast grating, concentrated photovoltaic system, nanoimprint lithography, reactive ion etching

SHORT ABSTRACT:
The fabrication of high contrast gratings as the parallel spectrum splitting dispersive element in a concentrated photovoltaic system is demonstrated. Fabrication processes including nanoimprint lithography, TiO_2 sputtering and reactive ion etching are described. Reflectance measurement results are used to characterize the optical performance.

LONG ABSTRACT:
High contrast gratings are designed and fabricated and its application is proposed in a parallel spectrum splitting dispersive element that can improve the solar conversion efficiency of a concentrated photovoltaic system. The proposed system will also lower the solar cell cost in the concentrated photovoltaic system by replacing the expensive tandem solar cells with the cost-effective single junction solar cells. The structures and the parameters of high contrast gratings for the dispersive elements were numerically optimized. The large-area fabrication of high

contrast gratings was experimentally demonstrated using nanoimprint lithography and dry etching. The quality of grating material and the performance of the fabricated device were both experimentally characterized. By analyzing the measurement results, the possible side effects from the fabrication processes are discussed and several methods that have the potential to improve the fabrication processes are proposed, which can help to increase the optical efficiency of the fabricated devices.

INTRODUCTION:

Our modern society will not survive without moving a significant portion of energy consumption to renewable energy sources. To make this happen, we have to find a way to harvest renewable energy at a cost lower than petroleum-based energy sources in the near future. Solar energy is the most abundant renewable energy on earth. Despite that a lot of progresses have been made in solar energy harvesting, it is still very challenging to compete with petroleum-based energy sources. Improving the efficiency of solar cells is one of the most efficient ways to lower the system cost of solar energy harvesting.

Optical lenses and dish reflectors are usually used in most concentrated photovoltaic (CPV) systems[1] to achieve a high concentration of solar power incidence on the small-area solar cells, so it is economically viable to exploit expensive tandem multi-junction solar cells[2] in CPV systems, and to maintain a reasonable cost at the same time. However, for most non-concentrated photovoltaic systems, which usually require a large-area installment of solar cells, the high-cost tandem solar cells cannot be incorporated, although they usually have a broader solar spectrum response and a higher overall conversion efficiency than the single junction solar cells[3].

Recently, with the help of the parallel spectrum splitting optics (i.e. dispersive element), the parallel spectrum splitting photovoltaic technology[4] has made it possible that a similar or better spectrum coverage and conversion efficiency can be achieved without using the expensive tandem solar cells. The solar spectrum can be split into different bands and each band can be absorbed and converted to electricity by the specialized single-junction solar cells. In this way, the expensive tandem solar cells in CPV systems can be replaced by a parallel distribution of single-junction solar cells without any compromise on the performance.

The dispersive element that was designed in this report can be applied in a reflective CPV system (which is based on dish reflectors) to realize parallel spectrum splitting for the improved solar-electricity conversion efficiency and reduced cost. Multilayer high contrast gratings (HCG)[5] is used as the dispersive element by designing each layer of HCG to work as an optical band reflector. The structures and parameters of the dispersive element are numerically optimized. Moreover, the fabrication of high contrast gratings for the dispersive element by using dielectric (TiO_2) sputtering, nanoimprint lithography[6] and reactive ion etching is studied and demonstrated.

PROTOCOL:

1. Prepare the blank Polydimethylsiloxane (PDMS) substrate for nanoimprint mold

1.1) Silicon wafer treatment process

1.1.1) Clean a 4-inch silicon wafer by rinsing with acetone, methanol and isopropanol.

1.1.2) Blow it dry using the nitrogen gun.

1.1.3) Clean it using piranha solution (3:1 mixture of sulfuric acid with 30% hydrogen peroxide) by soaking inside for 15 min.

1.1.4) Rinse it with DI water. Blow dry using the nitrogen gun.

1.1.5) Place the wafer in a glass desiccator. Add a drop (20 drops = 1 mL) of releasing agent (Trichlorosilane) into the desiccator.

1.1.6) Pump down the desiccator until the gauge reads -762 Torr and wait for 5 h.

1.1.7) Take the wafer out, which has been treated with releasing agent.

1.2) Preparation of PDMS film (used as mold in nanoimprint)

1.2.1) Weigh 10 g of silicone elastomer base and 1 g of curing agent.

1.2.2) Add them in the same glass beaker.

1.2.3) Stir and mix with a glass rod for 5 min.

1.2.4) Put the mixture into a vacuum desiccator until the gauge reads -762 Torr to pump out all the trapped air bubbles.

1.2.5) Spread them evenly onto the treated 4-inch silicon wafer.

1.2.6) Bake the wafer with PDMS on top in the vacuum oven for 7 h at 80 °C to cure the PDMS film.

2. Prepare the nanoimprint mold (duplication from the master mold)

2.1) Spin twelve drops (20 drops = 1 mL) of UV curable resist (15.2%) on a clean blank silicon wafer for 30 s at 1500 rpm.

2.2) Carefully peel a piece of PDMS film off the treated silicon wafer.

2.3) Put the PDMS film onto the UV curable resist and let it absorb the UV resist for 5 min then peel it off.

2.4) Repeat 2.1 - 2.3 on the same PDMS film for two times. Absorb the UV resist for 3 min and 1 min respectively.

2.5) Place the PDMS film (after three-time UV resist absorption) onto a silicon master mold.

2.6) Put it into a chamber with nitrogen environment.

2.7) Turn on UV lamp to cure the sample for 5 min.

2.8) Peel off the PDMS film. The cured UV resist on the PDMS will keep the negative pattern of the master mold.

2.9) Use RF O_2 plasma to treat the PDMS mold. (RF power: 30 W, pressure: 260 mTorr, time: 1 min)

2.10) Place the PDMS mold in a vacuum chamber with one drop (20 drops = 1 mL) of releasing agent for 2 h.

3. Nanoimprint pattern transfer

3.1) Spin eight drops (20 drops = 1 mL) of PMMA (996k, 3.1%) on the substrate to be imprinted for 50 s at 3500 rpm.

3.2) Bake it on a hotplate for 5 min at 120 °C.

3.3) Wait for the sample to cool down.

3.4) Spin eight drops (20 drops = 1 mL) of UV curable resist (3.9%) on the same substrate.

3.5) Place the PDMS mold (prepared in step 2) onto the sample (with both UV resist and PMMA).

3.6) Put it into a chamber with nitrogen environment.

3.7) Turn on the UV lamp to cure for 5 min.

3.8) Peel the PDMS mold off the sample and the pattern on the PDMS mold gets transferred to the sample.

4. Cr lift-off process

4.1) Reactive ion etching residual layer of UV resist and PMMA

Note: The SOP for ICP machine can be found at https://www.nanocenter.umd.edu/equipment/fablab/sops/etch-07/Oxford%20Chlorine%20Etcher%20SOP.pdf

4.1.1) Log in RIE ICP machine.

4.1.2) Load a blank 4-inch silicon wafer. Run the clean recipe for 10 min.

4.1.3) Take the blank silicon wafer out.

4.1.4) Mount the sample on another clean silicon wafer and load it into the machine.

4.1.5) Run the UV resist etching recipe for 2 min (the recipe can be found in Table 1).

4.1.6) Take the sample out. Load a blank 4-inch silicon wafer. Re-run the clean recipe (can be found in Table 1) for 10 min.

4.1.7) Mount the sample on a clean silicon wafer and load it into the machine.

4.1.8) Run the PMMA etching recipe (can be found in Table 1) for 2 min.

Note: Now the residual resist has been etched and substrate is exposed.

4.2) Cr e-beam evaporation

4.2.1) Log into e-beam evaporator.

4.2.2) Load the Cr metal source and sample into the chamber.

4.2.3) Set the thickness (20 nm) and deposition rate (0.03 nm/s).

4.2.4) Pump the chamber until required vacuum (10^{-7} Torr) is reached.

4.2.5) Start the deposition process.

4.2.6) Take the sample out after the deposition finishes.

4.3) Cr lift-off procedure

4.3.1) Immerse the sample in acetone with ultrasonic agitation for 5 min.

4.3.2) Clean the sample by rinsing with acetone, methanol and isopropanol.

Note: The Cr evaporated on the resist will be lifted off and a Cr mask for substrate etching is formed.

5. TiO_2 deposition

5.1) Load sample.

5.2) Set the parameters for the direct current magnetron sputtering machine

5.2.1) Use a chamber pressure of 1.5 mTorr, Ar flow of 100 SCCM and a sputtering power of 130 W.

5.2.2) Use a temperature of 27 °C and a stage rotation speed of 20 rpm.

5.3) Start the sputter process and stop at desired thickness.

5.4) Take the sample out and anneal the TiO_2 film in oxygen environment at 300 °C for 3 h.

6. High contrast grating etching

6.1) Log in the inductively coupled plasma (ICP) reactive ion etching (RIE) machine.

6.2) TiO_2 etching

6.2.1) Load a blank 4-inch silicon wafer.

6.2.2) Start and run the clean recipe (can be found in Table 1) for 10 min.

6.2.3) Unload load the blank wafer and load the sample with Cr mask.

6.2.4) Set etching time. Start TiO_2 etching recipe. The etching process will automatically stop.

6.2.6) Unload the sample.

6.3) SiO_2 etching

6.3.1) Repeat step 5.2 except use the SiO_2 etching recipe.

7. Reflectance measurement

7.1) Log in and turn on the measurement system.

7.2) Place the reflectance standard mirror on the sample holder and align the optical path.

7.3) Calibrate the system for the 100% reflectance.

7.4) Take off the reflectance standard mirror and place the HCG.

7.5) Measure the reflectance of the HCG.

7.6) Save the data and log out of the measurement system.

REPRESENTATIVE RESULTS:

Figure 1 shows the implementation of the dispersive element (multilayer high contrast grating (HCG)) in a concentrated photovoltaic system. The sun light is first reflected by the primary mirror and impinges on the reflective dispersive element, where the beam is reflected and split into different bands of different wavelengths. Each band will impinge on a certain location on the solar cell array for the best absorption and conversion to electricity. The key to this system is the design and implementation of the dispersive element, which is composed of multiple layers of HCG.

Figure 2 shows the numerical optimization result for each layer in the dispersive element. The results was calculated by the finite-difference time-domain (FDTD)[7] based commercial simulation software "Lumerical" and further validated by rigorous coupled-wave analysis (RCWA)[8]. The refractive index of TiO_2 was from the SOPRA[9] online database. The optimized six-layer dispersive element can provide a total reflection of more than 90% over the entire solar spectrum.[10,11]

To demonstrate the broadband reflectance of HCG experimentally, one of the six layers in the dispersive element HCG structure is fabricated using nanoimprint fabrication. As shown in Figure 3, each grating block consists of two parts. The material of the top grating is TiO_2 and the material of the sub grating is fused silica. The pitch of the 2D HCG is 453 nm. The line width of each grating is 220 nm. The height of both top and sub grating is 340 nm. The material of the substrate is the same as the sub grating.

TiO_2 was deposited on fused silica at HP Labs using a direct current magnetron sputter machine. The chamber pressure was 1.5 mTorr with an Ar flow about 100 sccm. The sputter power was 130 W and the rate was 4 nm/min. Two batches of TiO_2 film were sputtered at different temperatures, 27 °C and 270 °C respectively. To ensure an even film deposition, substrate stage rotation was turned on (20 rpm) during sputtering. Both batches of TiO_2 films were annealed at 300 °C for 3 hours after sputtering to improve film quality. After deposition, both batches of TiO_2 films were examined using a scanning electron microscope (SEM) (Figure 4). The refractive indices of TiO_2 films were also measured (Figure 5). The measured refractive indices were 10% lower than standard database, because the film was porous which can also be observed in Figure 4. A higher sputtering temperature could increase the refractive index, however the roughness of the film was much higher. To reach a good balance between refractive indices and film roughness, the TiO_2 film which was sputtered at 27 °C was chosen as the grating material.

The major steps for nanoimprint fabrication are schematically shown in Figure 6. First, a mold with certain patterns is pressed onto the UV-curable resist on the substrate. Then UV light is applied to cure the resist. After curing, the mold can be separated from the substrate and the shape of resist is exactly the opposite of the mold. The imprinted pattern can be used as the mask to etch the residual resist, deposit metal, lift off and finally etch into the substrate. In this way, the shape of the mold gets transferred into the substrate.

To fabricate 2D HCG, a mold is duplicated from a 1D periodic grating silicon master which was fabricated by interference lithography[12]. Then the same mold is used to imprint twice in orthogonal directions on the same silicon substrate to pattern a 2D hole array (Figure 7). The hybrid nanoimprint[13] process can make large-area samples with high-resolution and little defects. The imprinted results (2D hole array silicon array) is shown in Figure 8. The roughness of edges can be further reduced with the help of edge smoothing technologies[14].

After nanoimprint patterning and Cr mask array is completed, an ICP RIE machine is used to etch the sample. Two different etching recipes were developed for TiO_2 and fused silica respectively, which is shown in table 1. The fabricated structure is shown in Figure 9.

The reflectance (from the normal incidence) of 2D HCG was measured using two different spectrometers with different types of detectors, the normal detector and the sphere integration detector. In contrast to sphere integration detector, the normal detector has a relatively small angle of acceptance and therefore will not receive the scattered light. As shown in Figure 10, the difference in reflectance curves measured by both detectors indicates that the light is scattered by the HCG due to the structure roughness. The difference between integration sphere measurement and simulation data is mainly due to the loss of material and fabrication errors. The reflectance curves can demonstrate that the fabricated device can work as a band reflector as one layer in the dispersive element. Due to the high contrast of index between the grating and the substrate, HCG has good angle independence. The reflectance curve will not change much when the incidence angle is less than 15°.

Figure 1: The implementation of the dispersive element (multiplayer HCG) in a concentrated photovoltaic (CPV) system

Figure 2: Numerically optimized reflectance curves for the dispersive element design (six-layer stacked HCG) that can cover most of the solar spectrum

Figure 3: The optimized structure of a HCG for demonstration of nanoimprint fabrication

Figure 4: The SEM images (cross-sectional view) of sputtered TiO_2 films at (a) 27 °C and (b) 270 °C

Figure 5: Measured and standard refractive (SOPRA database) indices of sputtered TiO_2 films

Figure 6: Nanoimprint fabrication process

Figure 7: The SEM image of 2D hole array silicon master (top-down view)

Figure 8: The photo of 2D hole array silicon master fabricated by PDMS-based nanoimprint

Figure 9: The SEM image (cross-sectional view) of the fabricated 2D HCG

Figure 10: One simulated reflectance curve and two measured reflectance curves using sphere integration detector and normal detector respectively

Figure 11: (a) Effect of refractive index on HCG reflectance; (b) Effect of sidewall angle on HCG reflectance

Table 1: The table of etching recipes for TiO_2, fused silica, UV resist, PMMA and clean.

DISCUSSION:

First, the quality of the TiO_2 film is very crucial for the HCG performance. The reflectance peak will be higher if the TiO_2 film has less loss and surface roughness. The TiO_2 film with a higher refractive index is also favorable because the optical mode confinement will be enhanced by a higher contrast in index, which can give rise to a flatter and broader reflectance band in HCG.

Second, the fabrication errors will have significant effects on the HCG and should be avoided. The roughness introduced in fabrication will cause more light to be scattered, so the reflectance will become lower. The deviation of parameters in HCG fabrication including line width, height and pitch will not allow the device to work optimally as in simulation. Moreover, the reflectance of HCG strongly depends on the etching profile, i.e. the angle of sidewall. In Figure 11, the effect of sidewall angles on the reflectance of HCG is numerically calculated. As the sidewall angles decrease from 90° to 84°, the average reflectance drops from over 90% to less than 50%, because the HCG behaves more like a cone-shaped anti-reflection coating when the sidewall angle is small.

The optical efficiency of the dispersive element is important for the overall efficiency of the CPV system, so the reflectance of each layer of HCG should be as high as possible. Based on the discussion above, while the optical efficiency for the fabricated layer is about 60%, there are several possible improvements for a better HCG reflectance. The TiO_2 sputtering condition can be further optimized to generate the film with a higher index, less surface roughness and lower optical loss. The dry etching recipes should be further adjusted for a better etching profile, making the grating straighter, which can be achieved by adjusting the combination of gases (C_4F_8, $SF_6$and O_2) to balance the etching and re-deposition process. The nanoimprint and lift-off process should be improved to avoid roughness and fabrication errors so that the unnecessary scattering can be reduced to increase the overall optical efficiency.

By stacking multiple layers of two-dimensional HCGs with different pitches, the dispersive mirror can operate in much broader spectrum. The mirror can reflectively direct light into different angles according to wavelengths, in a way of packaging all HCG layers subsequently in different tilting angles. Moreover, the dispersive mirror can be fabricated using nanoimprint lithography (NIL) in a large area and at a low cost. Moreover, the proposed system features an easy integration with existing concentrator photovoltaic (CPV) setup so it has the potential to be accepted widely by the industry to improve solar energy conversion efficiency.

DISCLOSURES:

The authors have nothing to disclose.

ACKNOWLEDGMENTS:

This research was supported as part of the Center for Energy Nanoscience, an Energy Frontier Research Center funded by the U.S. Department of Energy, Office of Science under Award Number DE-SC0001013. We also want to thank Dr. Max Zhang and Dr. Jianhua Yang of HP Labs for their help on TiO_2 film sputtering and refractive indices measurement.

REFERENCES:

1 Horne, S. *et al.* A Solid 500 Sun Compound Concentrator PV Design. *Photovoltaic Energy Conversion, Conference Record of the 2006 IEEE 4th World Conference on.* 694-697, doi: 10.1109/WCPEC.2006.279550 (2006) .

2 Guter, W. *et al.* Current-matched triple-junction solar cell reaching 41.1% conversion efficiency under concentrated sunlight. *Applied Physics Letters* **94**, 223504 , doi: 10.1063/1.3148341 (2009).

3 Shockley, W. & Queisser, H. J. Detailed Balance Limit of Efficiency of p-n Junction Solar Cells. *Journal of Applied Physics* **32**, 510-519, doi: 10.1063/1.1736034 (1961).

4 Green, M. A. Potential for low dimensional structures in photovoltaics. *Materials Science and Engineering: B* **74**, 118-124, doi: 10.1016/S0921-5107(99)00546-2 (2000).

5 Karagodsky, V. & Chang-Hasnain, C. J. Physics of near-wavelength high contrast gratings. *Opt. Express* **20**, 10888-10895, doi: 10.1364/OE.20.010888 (2012).

6 Chou, S. Y., Krauss, P. R. & Renstrom, P. J. Nanoimprint lithography. *Journal of Vacuum Science & Technology B: Microelectronics and Nanometer Structures* **14**, 4129-4133, doi: 10.1116/1.588605 (1996).

7 Namiki, T. A new FDTD algorithm based on alternating-direction implicit method. *Microwave Theory and Techniques, IEEE Transactions on* **47**, 2003-2007, doi: 10.1109/22.795075 (1999).

8 Moharam, M. G. & Gaylord, T. K. Rigorous coupled-wave analysis of planar-grating diffraction. *J. Opt. Soc. Am.* **71**, 811-818, doi: 10.1364/josa.71.000811 (1981).

9 Smilab, S. nk Database. *World Wide Web:* http://www.sopra-sa.com (2015).

10 Yao, Y., Liu, H. & Wu, W. Spectrum splitting using multi-layer dielectric meta-surfaces for efficient solar energy harvesting. *Appl. Phys. A* **115**, 713-719, doi: 10.1007/s00339-014-8419-y (2014).

11 Yao, Y., Liu, H. & Wu, W. Fabrication of high-contrast gratings for a parallel spectrum splitting dispersive element in a concentrated photovoltaic system. *Journal of Vacuum Science & Technology B* **32**, 06FG04-06FG04-6, doi: 10.1116/1.4898198 (2014).

12 Solak, H. H. *et al.* Sub-50 nm period patterns with EUV interference lithography.

Microelectronic Engineering **67**, 56-62, doi: 10.1016/S0167-9317(03)00059-5 (2003).

13 Li, Z. *et al.* Hybrid nanoimprint− soft lithography with sub-15 nm resolution. *Nano letters* **9**, 2306-2310, doi: 10.1021/nl9004892 (2009).

14 Yu, Z., Chen, L., Wu, W., Ge, H. & Chou, S. Y. Fabrication of nanoscale gratings with reduced line edge roughness using nanoimprint lithography. *Journal of Vacuum Science & Technology B* **21**, 2089-2092, doi: 10.1116/1.1609471 (2003).

Figure1
Click here to download high resolution image

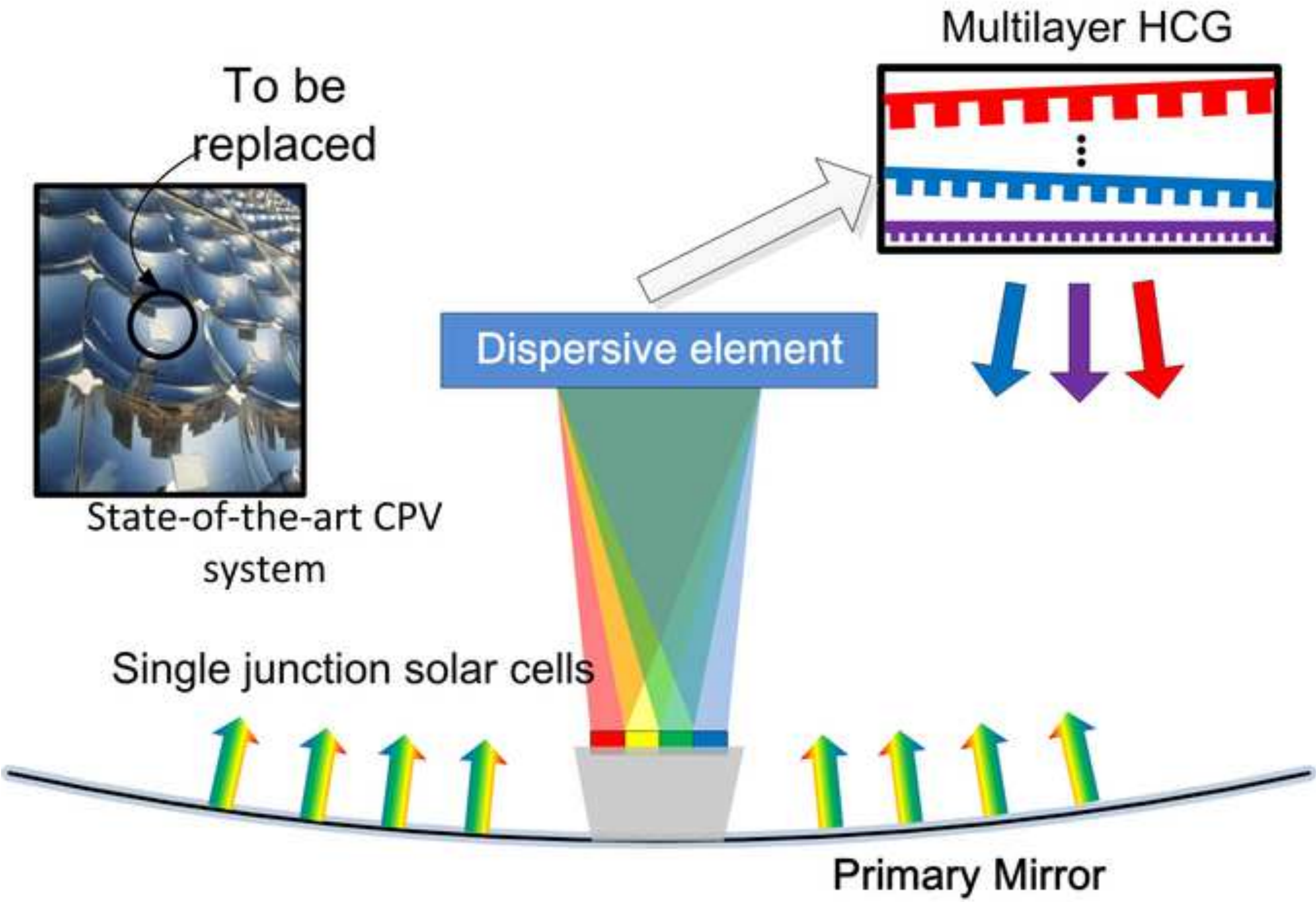

Figure2
Click here to download high resolution image

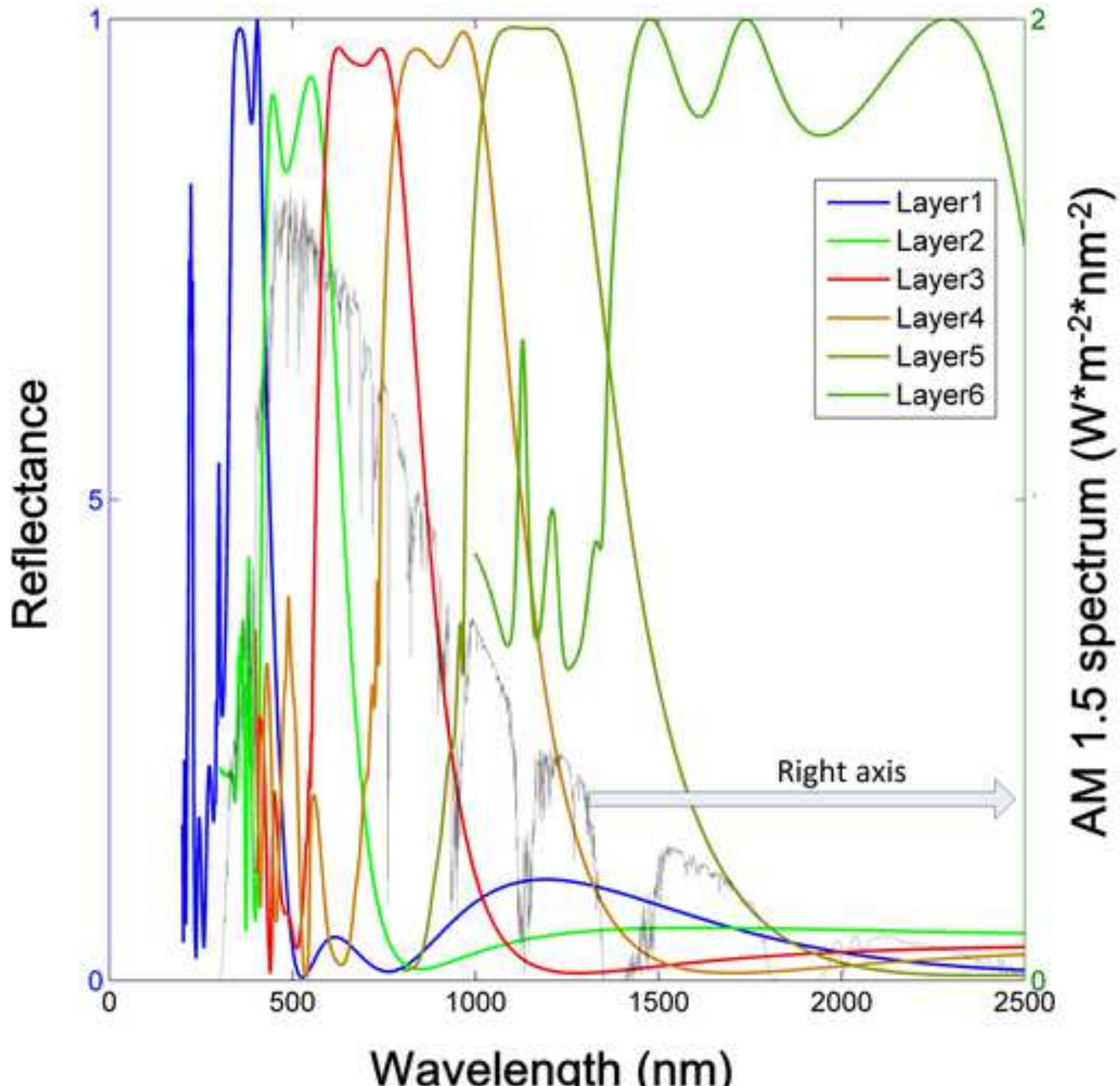

Figure3

Click here to download high resolution image

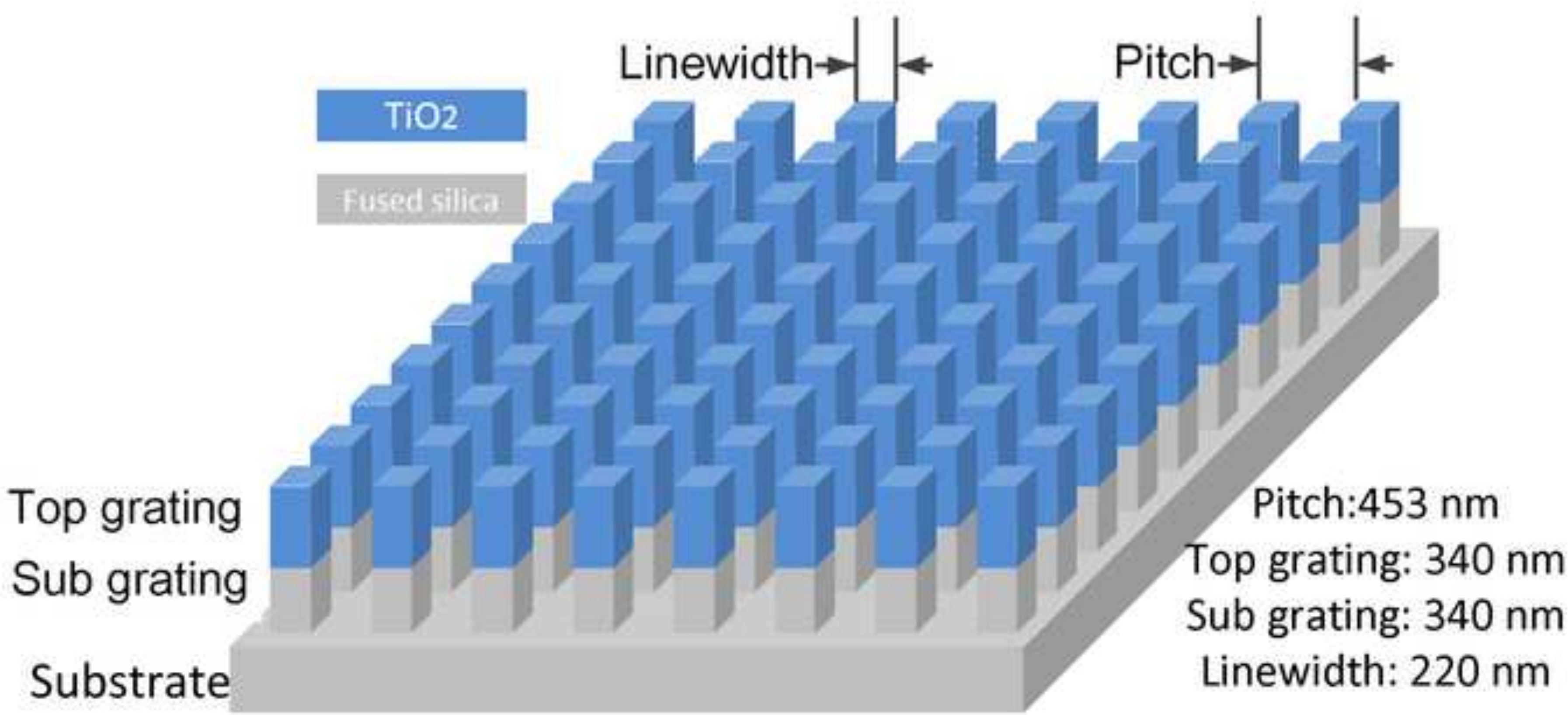

Figure4
Click here to download high resolution image

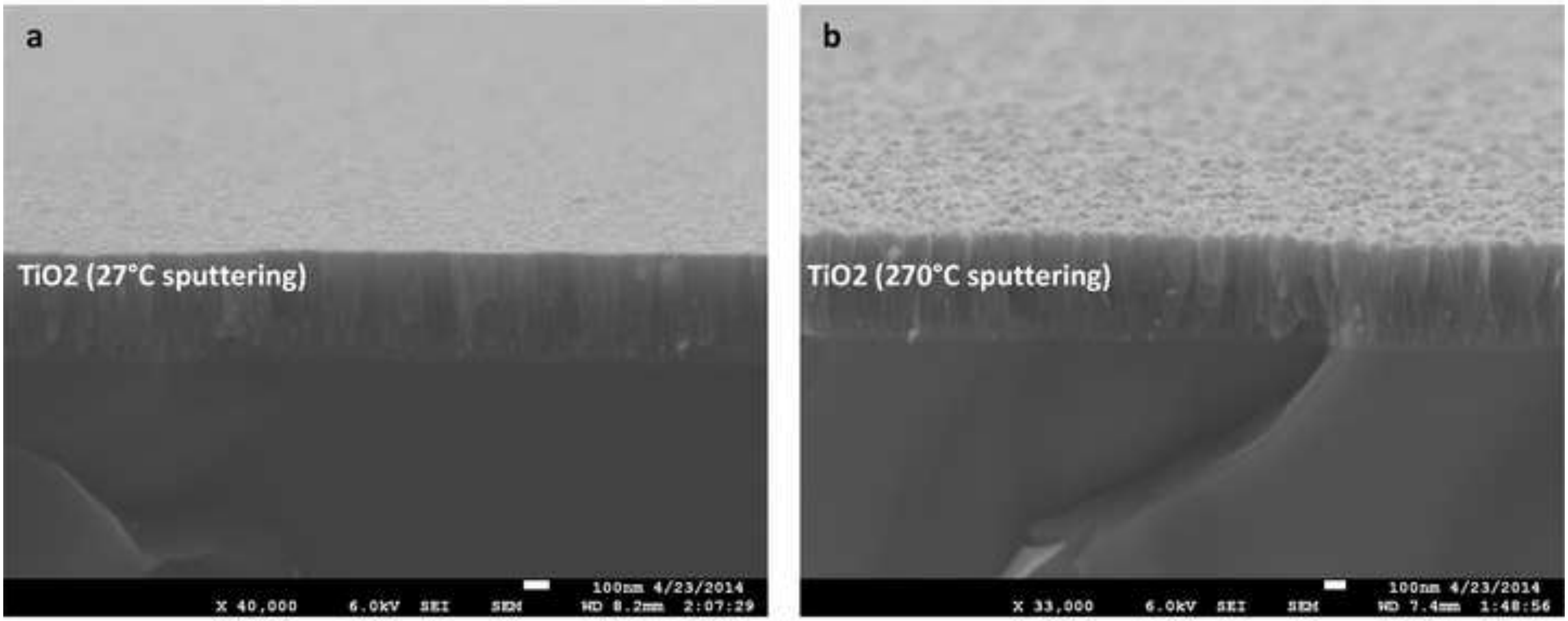

Figure5
Click here to download high resolution image

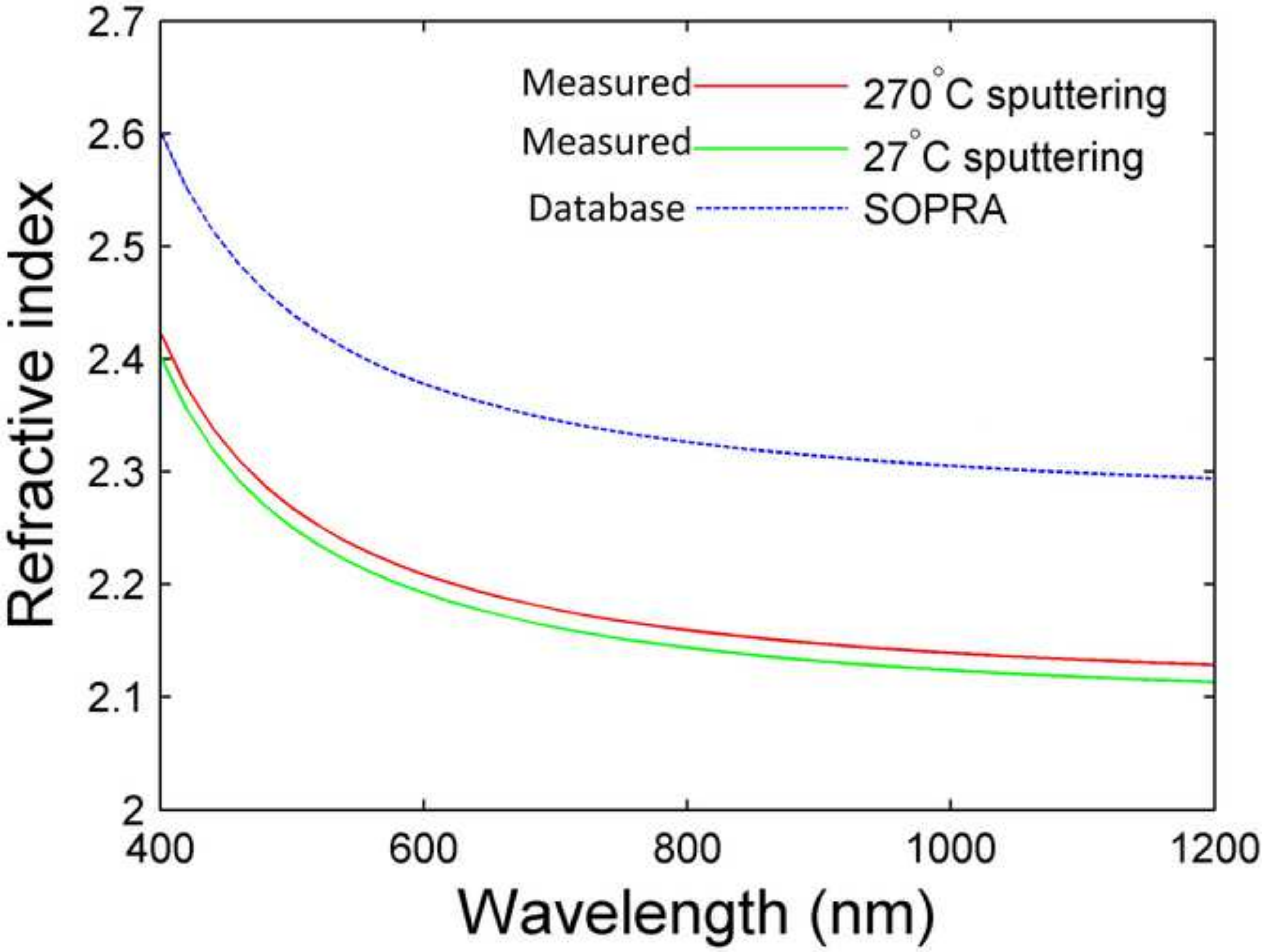

Figure6
Click here to download high resolution image

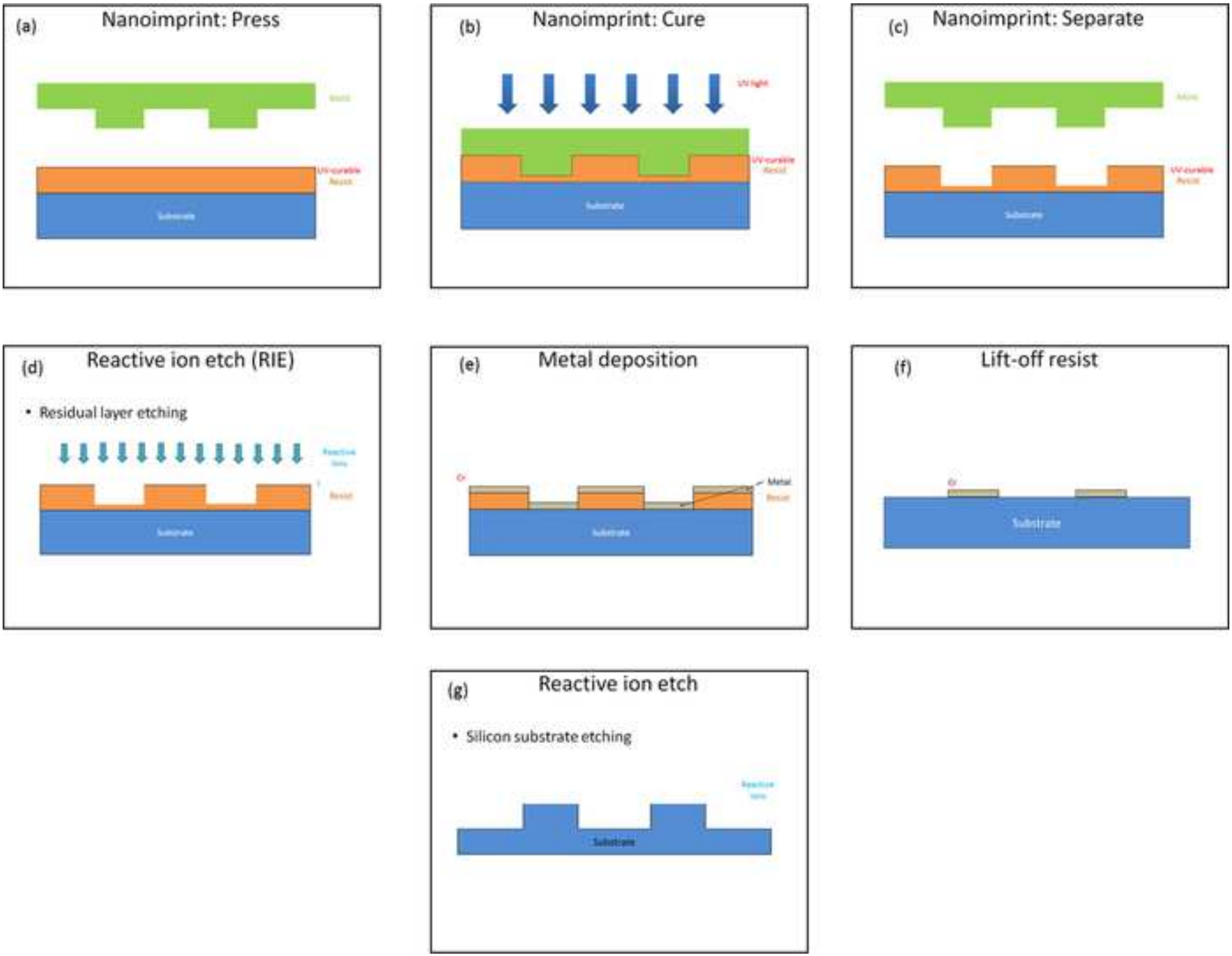

Figure7

Click here to download high resolution image

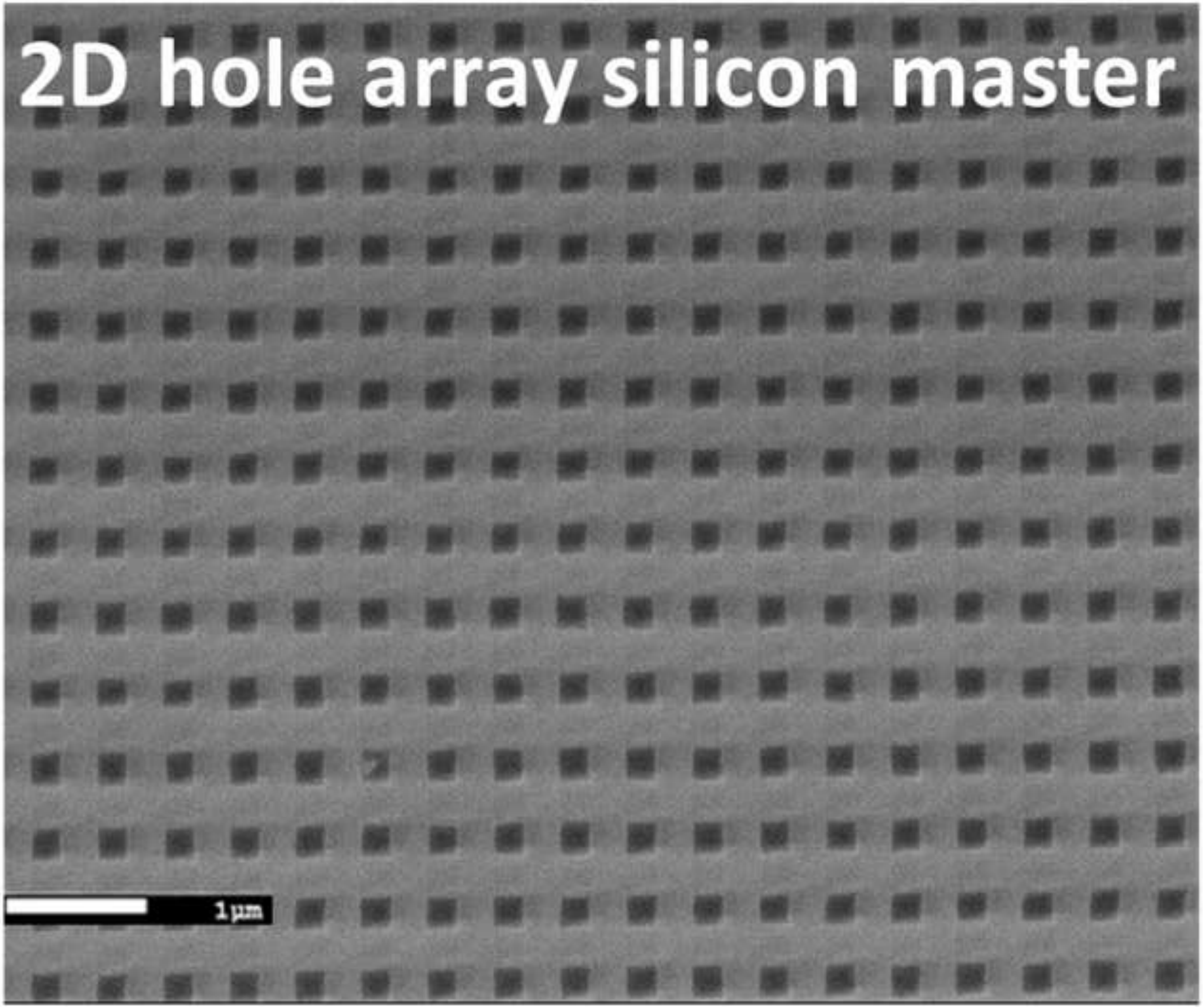

Figure8

Click here to download high resolution image

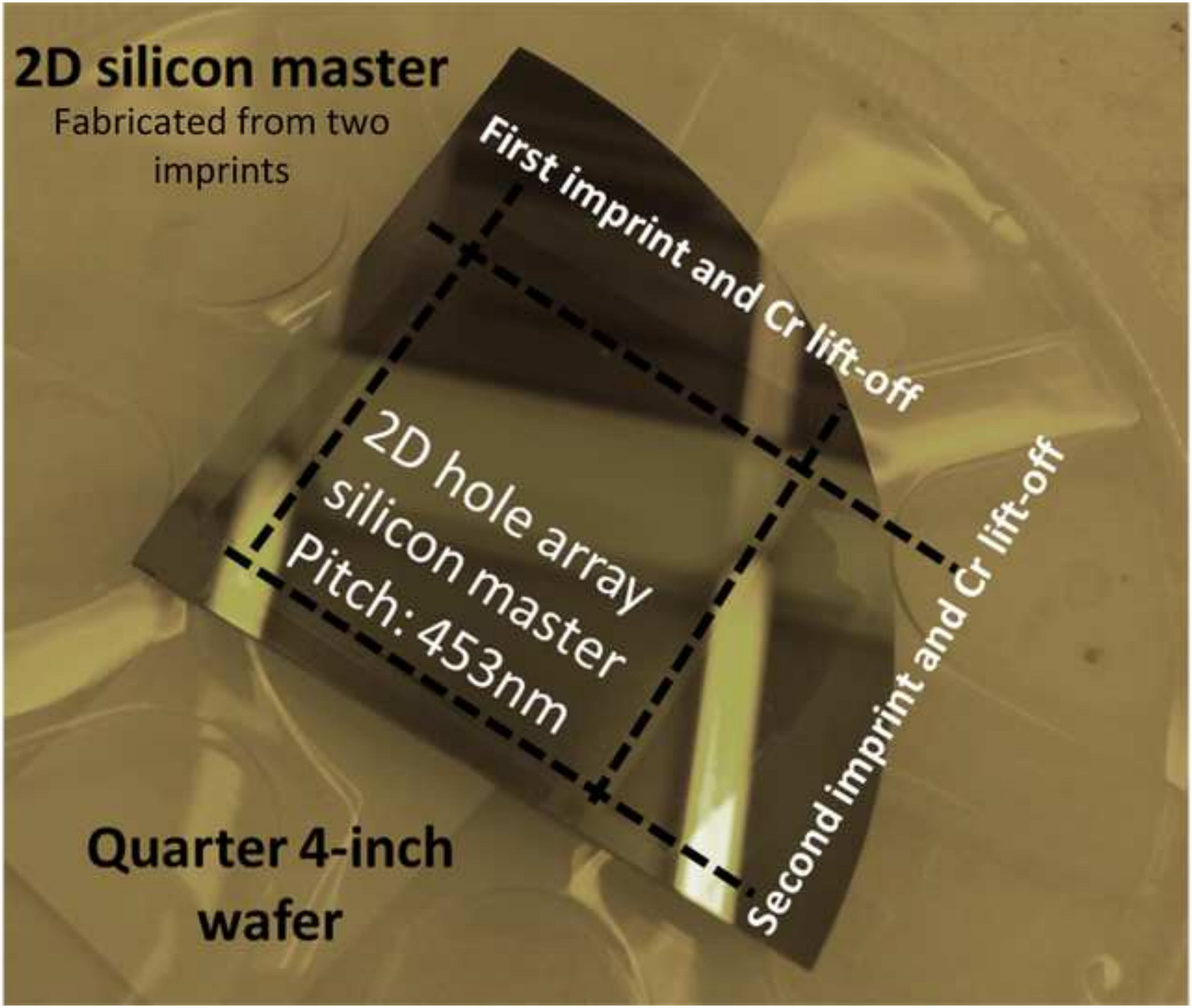

Figure9

Click here to download high resolution image

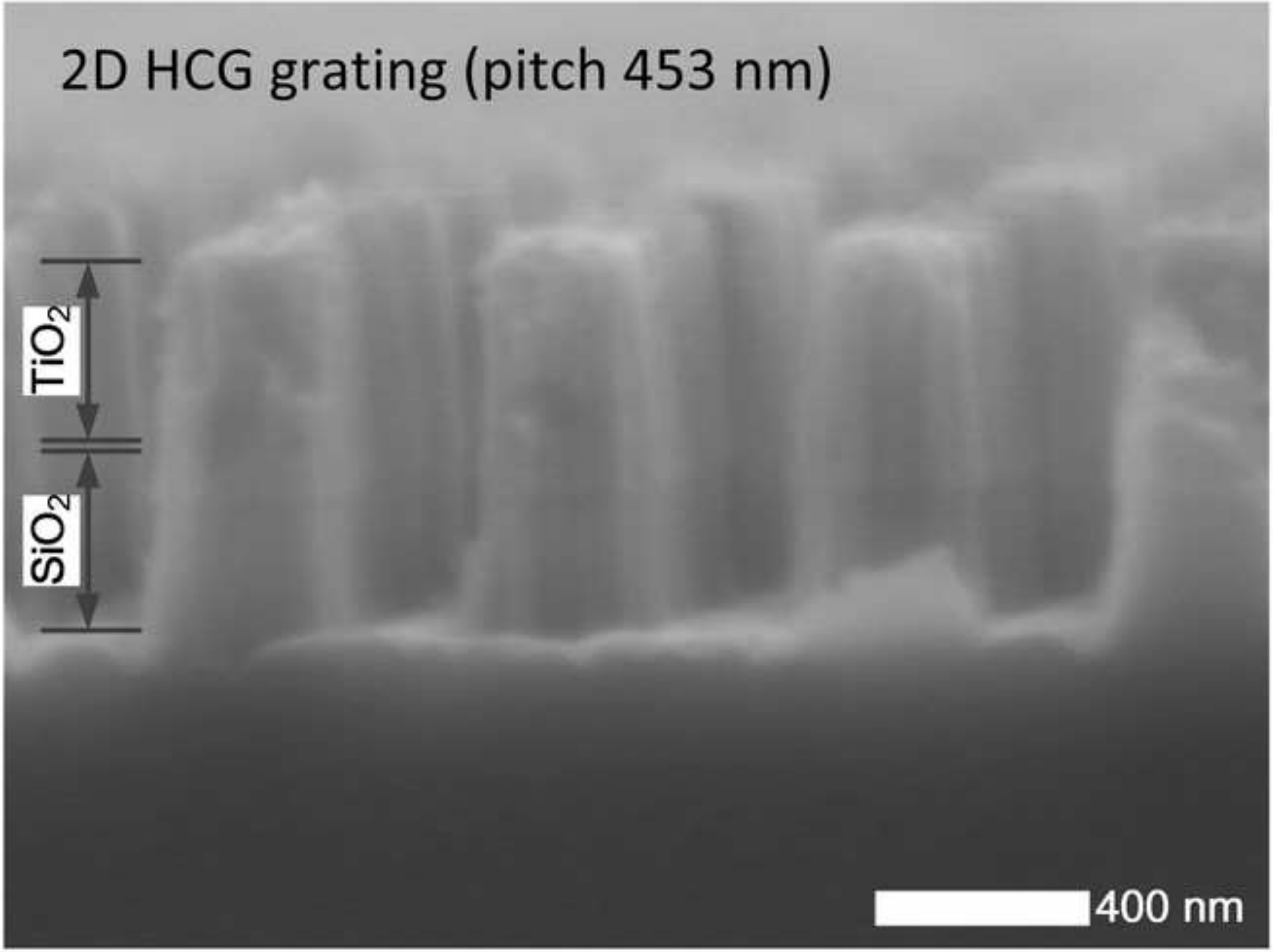

Figure10
Click here to download high resolution image

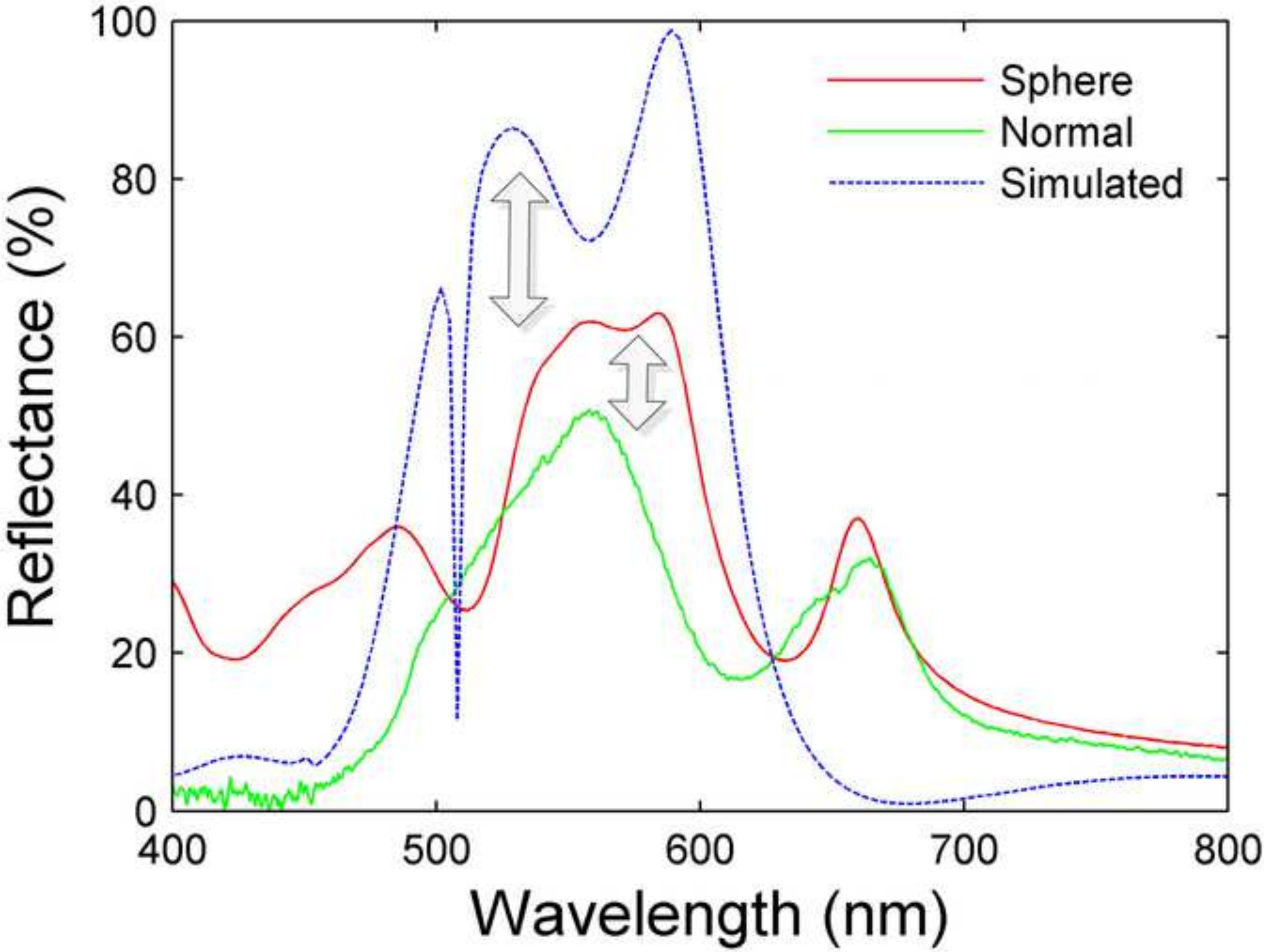

Figure11
Click here to download high resolution image

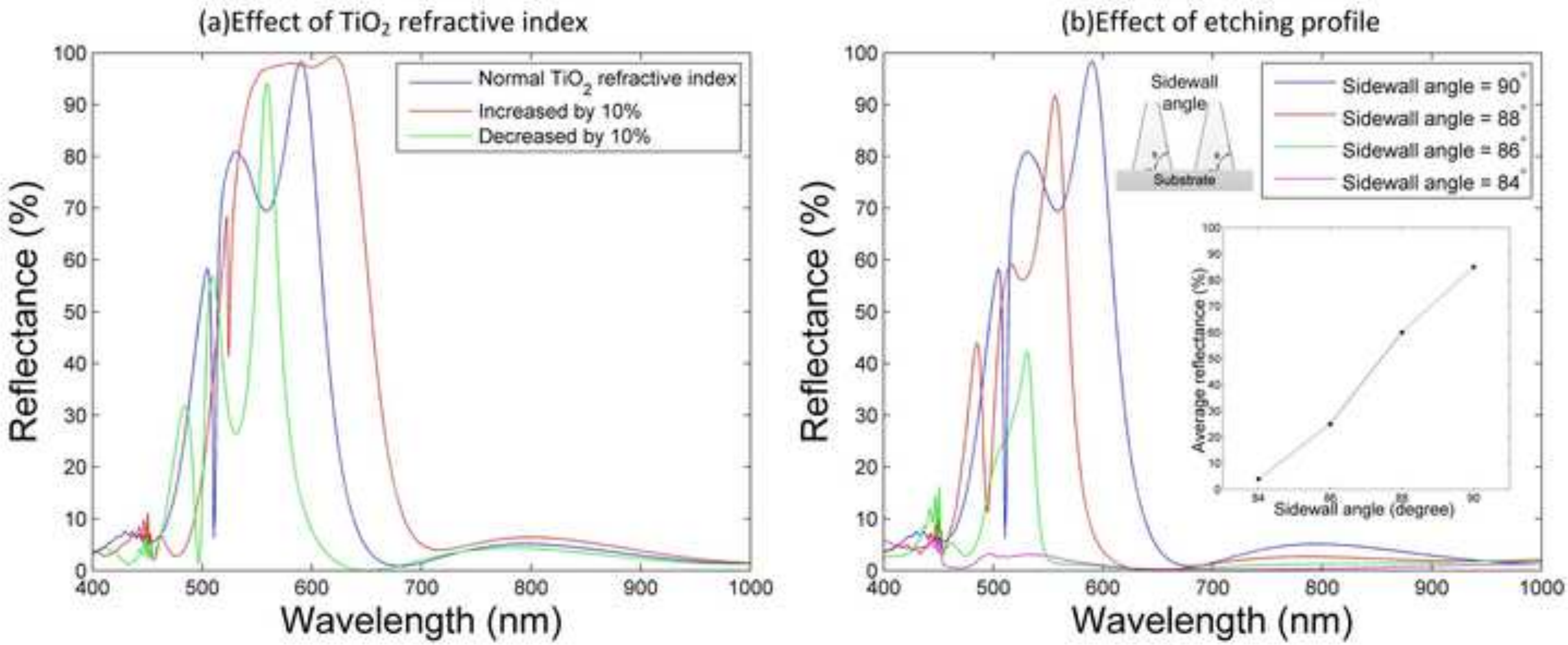

Table2_Excel Spreadsheet- Table of Materials/Equipment

Click here to download Excel Spreadsheet- Table of Materials/Equipment: table2_JoVE_Materials.xls

Name of Material/ Equipment	Company	Catalog Number
184 SILICONE ELASTOMER KIT	SYLGARD	
4-inch silicon wafer	Universitywafer	
4-inch fused silica wafer	Universitywafer	
Poly(methyl methacrylate)	SIGMA-ALDRICH	182265
UV-curable resist		
PlasmaLab System 100	Oxford Instruments	
UV curing system for nanoimprint fabrication		
Ocean Optics HR-4000	Ocean Optics	HR-4000
Lambda 950 UV / VIS	PerkinElmer	
JSM-7001F-LV	JEOL	
DC magnetron sputtering machine		
Metal e-beam evaporator	Temescal	BJD-1800

Comments/Description

Polydimethylsiloxane (PDMS)

Nor available on market
ICP IRE machine
Not available on market
Spectrometer with normal detector
spectrometer with hemisphere intergration detector
Field emission SEM
Equipment is in HP labs, who helped us to sputter the TiO_2

Table 1 in excel

Click here to download Excel Spreadsheet- Table of Materials/Equipment: Table1.xlsx

	ICP Power	Forward Power	SF6 Flow	C4F8 Flow	O2 Flow	Pressure	Etching Rate
TiO_2	0 W	25 W	25 sccm	10 sccm	10 sccm	10mTorr	43nm/min
Fused silica	0 W	100 W	0 sccm	15 sccm	15 sccm	10mTorr	20nm/min
Resist	0 W	25 W	25 sccm	15 sccm	0	10mTorr	22nm/min
PMMA	0W	30W	0	0	30 sccm	2mTorr	55nm/min
Clean	1000W	200W	0	0	50 sccm	50mTorr	NA

JOURNAL OF VISUALIZED EXPERIMENTS
1 Alewife Center #200
Cambridge, MA 02140
tel. 617.945.9051
www.jove.com

ARTICLE AND VIDEO LICENSE AGREEMENT

Title of Article: Fabrication of high contrast gratings for the spectrum splitting dispersive element in a concentrated photovoltaic system

Author(s): Yuhan Yao, He Liu, Wei Wu

Item 1 (check one box): The Author elects to have the Materials be made available (as described at http://www.jove.com/publish) via: ☑ Standard Access ☐ Open Access

Item 2 (check one box):

☑ The Author is NOT a United States government employee.

☐ The Author is a United States government employee and the Materials were prepared in the course of his or her duties as a United States government employee.

☐ The Author is a United States government employee but the Materials were NOT prepared in the course of his or her duties as a United States government employee.

ARTICLE AND VIDEO LICENSE AGREEMENT

1. Defined Terms. As used in this Article and Video License Agreement, the following terms shall have the following meanings: "**Agreement**" means this Article and Video License Agreement; "**Article**" means the article specified on the last page of this Agreement, including any associated materials such as texts, figures, tables, artwork, abstracts, or summaries contained therein; "**Author**" means the author who is a signatory to this Agreement; "**Collective Work**" means a work, such as a periodical issue, anthology or encyclopedia, in which the Materials in their entirety in unmodified form, along with a number of other contributions, constituting separate and independent works in themselves, are assembled into a collective whole; "**CRC License**" means the Creative Commons Attribution-Non Commercial-No Derivs 3.0 Unported Agreement, the terms and conditions of which can be found at: http://creativecommons.org/licenses/by-nc-nd/3.0/legalcode; "**Derivative Work**" means a work based upon the Materials or upon the Materials and other pre-existing works, such as a translation, musical arrangement, dramatization, fictionalization, motion picture version, sound recording, art reproduction, abridgment, condensation, or any other form in which the Materials may be recast, transformed, or adapted; "**Institution**" means the institution, listed on the last page of this Agreement, by which the Author was employed at the time of the creation of the Materials; "**JoVE**" means MyJove Corporation, a Massachusetts corporation and the publisher of *The Journal of Visualized Experiments;* "**Materials**" means the Article and / or the Video; "**Parties**" means the Author and JoVE; "**Video**" means any video(s) made by the Author, alone or in conjunction with any other parties, or by JoVE or its affiliates or agents, individually or in collaboration with the Author or any other parties, incorporating all or any portion of the Article, and in which the Author may or may not appear.

2. Background. The Author, who is the author of the Article, in order to ensure the dissemination and protection of the Article, desires to have the JoVE publish the Article and create and transmit videos based on the Article. In furtherance of such goals, the Parties desire to memorialize in this Agreement the respective rights of each Party in and to the Article and the Video.

3. Grant of Rights in Article. In consideration of JoVE agreeing to publish the Article, the Author hereby grants to JoVE, subject to **Sections 4** and **7** below, the exclusive, royalty-free, perpetual (for the full term of copyright in the Article, including any extensions thereto) license (a) to publish, reproduce, distribute, display and store the Article in all forms, formats and media whether now known or hereafter developed (including without limitation in print, digital and electronic form) throughout the world, (b) to translate the Article into other languages, create adaptations, summaries or extracts of the Article or other Derivative Works (including, without limitation, the Video) or Collective Works based on all or any portion of the Article and exercise all of the rights set forth in (a) above in such translations, adaptations, summaries, extracts, Derivative Works or Collective Works and (c) to license others to do any or all of the above. The foregoing rights may be exercised in all media and formats, whether now known or hereafter devised, and include the right to make such modifications as are technically necessary to exercise the rights in other media and formats. If the "Open Access" box has been checked in **Item 1** above, JoVE and the Author hereby grant to the public all such rights in the Article as provided in, but subject to all limitations and requirements set forth in, the CRC License.

JOURNAL OF VISUALIZED EXPERIMENTS
1 Alewife Center #200
Cambridge, MA 02140
tel. 617.945.9051
www.jove.com

ARTICLE AND VIDEO LICENSE AGREEMENT

4. Retention of Rights in Article. Notwithstanding the exclusive license granted to JoVE in **Section 3** above, the Author shall, with respect to the Article, retain the non-exclusive right to use all or part of the Article for the non-commercial purpose of giving lectures, presentations or teaching classes, and to post a copy of the Article on the Institution's website or the Author's personal website, in each case provided that a link to the Article on the JoVE website is provided and notice of JoVE's copyright in the Article is included. All non-copyright intellectual property rights in and to the Article, such as patent rights, shall remain with the Author.

5. Grant of Rights in Video – Standard Access. This **Section 5** applies if the "Standard Access" box has been checked in **Item 1** above or if no box has been checked in **Item 1** above. In consideration of JoVE agreeing to produce, display or otherwise assist with the Video, the Author hereby acknowledges and agrees that, Subject to **Section 7** below, JoVE is and shall be the sole and exclusive owner of all rights of any nature, including, without limitation, all copyrights, in and to the Video. To the extent that, by law, the Author is deemed, now or at any time in the future, to have any rights of any nature in or to the Video, the Author hereby disclaims all such rights and transfers all such rights to JoVE.

6. Grant of Rights in Video – Open Access. This **Section 6** applies only if the "Open Access" box has been checked in **Item 1** above. In consideration of JoVE agreeing to produce, display or otherwise assist with the Video, the Author hereby grants to JoVE, subject to **Section 7** below, the exclusive, royalty-free, perpetual (for the full term of copyright in the Article, including any extensions thereto) license (a) to publish, reproduce, distribute, display and store the Video in all forms, formats and media whether now known or hereafter developed (including without limitation in print, digital and electronic form) throughout the world, (b) to translate the Video into other languages, create adaptations, summaries or extracts of the Video or other Derivative Works or Collective Works based on all or any portion of the Video and exercise all of the rights set forth in (a) above in such translations, adaptations, summaries, extracts, Derivative Works or Collective Works and (c) to license others to do any or all of the above. The foregoing rights may be exercised in all media and formats, whether now known or hereafter devised, and include the right to make such modifications as are technically necessary to exercise the rights in other media and formats. For any Video to which this Section 6 is applicable, JoVE and the Author hereby grant to the public all such rights in the Video as provided in, but subject to all limitations and requirements set forth in, the CRC License.

7. Government Employees. If the Author is a United States government employee and the Article was prepared in the course of his or her duties as a United States government employee, as indicated in **Item 2** above, and any of the licenses or grants granted by the Author hereunder exceed the scope of the 17 U.S.C. 403, then the rights granted hereunder shall be limited to the maximum rights permitted under such statute. In such case, all provisions contained herein that are not in conflict with such statute shall remain in full force and effect, and all provisions contained herein that do so conflict shall be deemed to be amended so as to provide to JoVE the maximum rights permissible within such statute.

8. Likeness, Privacy, Personality. The Author hereby grants JoVE the right to use the Author's name, voice, likeness, picture, photograph, image, biography and performance in any way, commercial or otherwise, in connection with the Materials and the sale, promotion and distribution thereof. The Author hereby waives any and all rights he or she may have, relating to his or her appearance in the Video or otherwise relating to the Materials, under all applicable privacy, likeness, personality or similar laws.

9. Author Warranties. The Author represents and warrants that the Article is original, that it has not been published, that the copyright interest is owned by the Author (or, if more than one author is listed at the beginning of this Agreement, by such authors collectively) and has not been assigned, licensed, or otherwise transferred to any other party. The Author represents and warrants that the author(s) listed at the top of this Agreement are the only authors of the Materials. If more than one author is listed at the top of this Agreement and if any such author has not entered into a separate Article and Video License Agreement with JoVE relating to the Materials, the Author represents and warrants that the Author has been authorized by each of the other such authors to execute this Agreement on his or her behalf and to bind him or her with respect to the terms of this Agreement as if each of them had been a party hereto as an Author. The Author warrants that the use, reproduction, distribution, public or private performance or display, and/or modification of all or any portion of the Materials does not and will not violate, infringe and/or misappropriate the patent, trademark, intellectual property or other rights of any third party. The Author represents and warrants that it has and will continue to comply with all government, institutional and other regulations, including, without limitation all institutional, laboratory, hospital, ethical, human and animal treatment, privacy, and all other rules, regulations, laws, procedures or guidelines, applicable to the Materials, and that all research involving human and animal subjects has been approved by the Author's relevant institutional review board.

10. JoVE Discretion. If the Author requests the assistance of JoVE in producing the Video in the Author's facility, the Author shall ensure that the presence of JoVE employees, agents or independent contractors is in accordance with the relevant regulations of the Author's institution. If more than one author is listed at the beginning of this Agreement, JoVE may, in its sole discretion, elect not take any action with respect to the Article until such time as it has received complete, executed Article and Video License Agreements from each such author. JoVE reserves the right, in its absolute and sole discretion and without giving any reason therefore, to accept or decline any work submitted to JoVE. JoVE and its employees, agents and independent contractors shall have

ARTICLE AND VIDEO LICENSE AGREEMENT

full, unfettered access to the facilities of the Author or of the Author's institution as necessary to make the Video, whether actually published or not. JoVE has sole discretion as to the method of making and publishing the Materials, including, without limitation, to all decisions regarding editing, lighting, filming, timing of publication, if any, length, quality, content and the like.

11. Indemnification. The Author agrees to indemnify JoVE and/or its successors and assigns from and against any and all claims, costs, and expenses, including attorney's fees, arising out of any breach of any warranty or other representations contained herein. The Author further agrees to indemnify and hold harmless JoVE from and against any and all claims, costs, and expenses, including attorney's fees, resulting from the breach by the Author of any representation or warranty contained herein or from allegations or instances of violation of intellectual property rights, damage to the Author's or the Author's institution's facilities, fraud, libel, defamation, research, equipment, experiments, property damage, personal injury, violations of institutional, laboratory, hospital, ethical, human and animal treatment, privacy or other rules, regulations, laws, procedures or guidelines, liabilities and other losses or damages related in any way to the submission of work to JoVE, making of videos by JoVE, or publication in *JoVE* or elsewhere by JoVE. The Author shall be responsible for, and shall hold JoVE harmless from, damages caused by lack of sterilization, lack of cleanliness or by contamination due to the making of a video by JoVE its employees, agents or independent contractors. All sterilization, cleanliness or decontamination procedures shall be solely the responsibility of the Author and shall be undertaken at the Author's expense. All indemnifications provided herein shall include JoVE's attorney's fees and costs related to said losses or damages. Such indemnification and holding harmless shall include such losses or damages incurred by, or in connection with, acts or omissions of JoVE, its employees, agents or independent contractors.

12. Fees. To cover the cost incurred for publication, JoVE must receive payment before production and publication the Materials. Payment is due in 21 days of invoice. Should the Materials not be published due to an editorial or production decision, these funds will be returned to the Author. Withdrawal by the Author of any submitted Materials after final peer review approval will result in a US$1,200 fee to cover pre-production expenses incurred by JoVE. If payment is not received by the completion of filming, production and publication of the Materials will be suspended until payment is received.

13. Transfer, Governing Law. This Agreement may be assigned by JoVE and shall inure to the benefits of any of JoVE's successors and assignees. This Agreement shall be governed and construed by the internal laws of the Commonwealth of Massachusetts without giving effect to any conflict of law provision thereunder. This Agreement may be executed in counterparts, each of which shall be deemed an original, but all of which together shall be deemed to me one and the same agreement. A signed copy of this Agreement delivered by facsimile, e-mail or other means of electronic transmission shall be deemed to have the same legal effect as delivery of an original signed copy of this Agreement.

A signed copy of this document must be sent with all new submissions. Only one Agreement required per submission.

CORRESPONDING AUTHOR:

Name: Wei Wu

Department: Department of Electrical Engineering - Electrophysics

Institution: University of Southern California

Article Title: Fabrication of high contrast gratings for the dispersive element in a concentrated photovoltaic system

Signature:

Date: 11/6/2014

Please submit a signed and dated copy of this license by one of the following three methods:

1) Upload a scanned copy of the document as a pfd on the JoVE submission site;
2) Fax the document to +1.866.381.2236;
3) Mail the document to JoVE / Attn: JoVE Editorial / 1 Alewife Center #200 / Cambridge, MA 02139

For questions, please email submissions@jove.com or call +1.617.945.9051

TITLE:

Fabrication of high contrast gratings for the spectrum splitting dispersive element in a concentrated photovoltaic system

AUTHORS:

Yao, Yuhan
Department of Electrical Engineering
University of Sothern California
Los Angeles, CA
yuhanyao@usc.edu

Liu, He
Department of Electrical Engineering
University of Sothern California
Los Angeles, CA
heliu@usc.edu

Wu, Wei
Department of Electrical Engineering
University of Sothern California
Los Angeles, CA
Wu.w@usc.edu

CORRESPONDING AUTHOR:

Wu, Wei

KEYWORDS:

Parallel spectrum splitting, dispersive element, high contrast grating, concentrated photovoltaic system, nanoimprint lithography, reactive ion etching

SHORT ABSTRACT:

The fabrication of high contrast gratings as the parallel spectrum splitting dispersive element in a concentrated photovoltaic system is demonstrated. Fabrication processes including nanoimprint lithography, TiO_2 sputtering and reactive ion dry etching are described. Reflectance measurement results are used to characterize the optical performance.

LONG ABSTRACT:

High contrast gratings are designed and fabricated and its application is proposed in a parallel spectrum splitting dispersive element that can improve the solar conversion efficiency of a concentrated photovoltaic system. The proposed system will also lower the solar cell cost in the concentrated photovoltaic system by replacing the expensive tandem solar cells with the cost-effective single junction solar cells. The structures and the parameters of high contrast gratings for the dispersive elements were numerically optimized. The large-area fabrication of high

contrast gratings was experimentally demonstrated using nanoimprint lithography and dry etching. The quality of grating material and the performance of the fabricated device were both experimentally characterized. By analyzing the measurement results, the possible side effects from the fabrication processes are discussed and several methods that have the potential to improve the fabrication processes are proposed, which can help to increase the optical efficiency of the fabricated devices.

INTRODUCTION:

Formatted: Font color: Black

Our modern society will not survive without moving a significant portion of energy consumption to renewable energy sources. To make this happen, we have to find a way to harvest renewable energy at a cost lower than petroleum-based energy sources in the near future. Solar energy is the most abundant renewable energy on earth. Despite that a lot of progresses have been made in solar energy harvesting, it is still very challenging to compete with petroleum-based energy sources. Improving the efficiency of solar cells is one of the most efficient ways to lower the system cost of solar energy harvesting.

Optical lenses and dish reflectors are usually used in most concentrated photovoltaic (CPV) systems[~~1~~1] to achieve a high concentration of solar power incidence on the small-area solar cells, so it is economically viable to exploit expensive tandem multi-junction solar cells[~~2~~2] in CPV systems, and to maintain a reasonable cost at the same time. However, for most non-concentrated photovoltaic systems, which usually require a large-area installment of solar cells, the high-cost tandem solar cells cannot be incorporated, although they usually have a broader solar spectrum response and a higher overall conversion efficiency than the single junction solar cells[~~3~~3].

Recently, with the help of the parallel spectrum splitting optics (i.e. dispersive element), the parallel spectrum splitting photovoltaic technology[~~4~~4] has made it possible that a similar or better spectrum coverage and conversion efficiency can be achieved without using the expensive tandem solar cells. The solar spectrum can be split into different bands and each band can be absorbed and converted to electricity by the specialized single-junction solar cells. In this way, the expensive tandem solar cells in CPV systems can be replaced by a parallel distribution of single-junction solar cells without any compromise on the performance.

The dispersive element that was designed in this report can be applied in a reflective CPV system (which is based on dish reflectors) to realize parallel spectrum splitting for the improved solar-electricity conversion efficiency and reduced cost. ~~Multilayer high contrast gratings (HCG)~~[5]Multilayer high contrast gratings (HCG)[5] is used as the dispersive element by designing each layer of HCG to work as an optical band reflector. The structures and parameters of the dispersive element are numerically optimized. Moreover, the fabrication of high contrast gratings for the dispersive element by using dielectric (TiO_2) sputtering, nanoimprint lithography[~~6~~6] and reactive ion etching is studied and demonstrated.

PROTOCOL:

1. Prepare the blank Polydimethylsiloxane (PDMS) substrate for nanoimprint mold

1.1) Silicon wafer treatment process

1.1.1) Clean a 4-inch silicon wafer by rinsing with acetone, methanol and isopropanol.

1.1.2) Blow it dry using the nitrogen gun.

1.1.3) Clean it using piranha solution (3:1 mixture of sulfuric acid with 30% hydrogen peroxide) by soaking inside for 15 min.

1.1.4) Rinse it with DI water. Blow dry using the nitrogen gun.

1.1.5) Place the wafer in a glass desiccator. Add a drop (20 drops = 1 mL) of releasing agent (Trichlorosilane) into the desiccator.

1.1.6) Pump down the desiccator until the gauge reads -30 inHg and wait for 5 hr.

1.1.7) Take the wafer out, which has been treated with releasing agent.

1.2) Preparation of PDMS film (used as mold in nanoimprint)

1.2.1) Weigh 10 g of silicone elastomer base and 1 g of curing agent.

1.2.2) Add them in the same glass beaker.

1.2.3) Stir and mix with a glass rod for 5 min.

1.2.4) Put the mixture into a vacuum desiccator until the gauge reads -30 inHg to pump out all the trapped air bubbles.

1.2.5) Spread them evenly onto the treated 4-inch silicon wafer.

1.2.6) Bake the wafer with PDMS on top in the vacuum oven for 7 hours at 80 °C to cure the PDMS film.

2. Prepare the nanoimprint mold (duplication from the master mold)

2.1) Spin twelve drops (20 drops = 1 mL) of UV curable resist (15.2%) on a clean blank silicon wafer for 30 s at 1500 rpm.

2.2) Carefully peel a piece of PDMS film off the treated silicon wafer.

2.3) Put the PDMS film onto the UV curable resist and let it absorb the UV resist for 5 min then peel it off.

2.4) Repeat 2.1 - 2.3 on the same PDMS film for two times. Absorb the UV resist for 3 min and 1 min respectively.

2.5) Place the PDMS film (after three-time UV resist absorption) onto a silicon master mold.

2.6) Put it into a chamber with nitrogen environment.

2.7) Turn on UV lamp to cure the sample for 5 min.

2.8) Peel off the PDMS film. The cured UV resist on the PDMS will keep the negative pattern of the master mold.

2.9) Use RF O_2 plasma to treat the PDMS mold. (RF power: 30 W, pressure: 260 mTorr, time: 1 min)

2.10) Place the PDMS mold in a vacuum chamber with one drop (20 drops = 1 mL) of releasing agent for 2 hr.

3. Nanoimprint pattern transfer

3.1) Spin eight drops (20 drops = 1 mL) of PMMA (996k, 3.1%) on the substrate to be imprinted for 50 s at 3500 rpm.

3.2) Bake it on a hotplate for 5 min at 120 °C.

3.3) Wait for the sample to cool down.

3.4) Spin eight drops (20 drops = 1 mL) of UV curable resist (3.9%) on the same substrate.

3.5) Place the PDMS mold (prepared in step 2) onto the sample (with both UV resist and PMMA).

3.6) Put it into a chamber with nitrogen environment.

3.7) Turn on the UV lamp to cure for 5 min.

3.8) Peel the PDMS mold off the sample and the pattern on the PDMS mold gets transferred to the sample.

4. Cr lift-off process

4.1) Reactive ion etching residual layer of UV resist and PMMA

Note: The SOP for ICP machine can be found at https://www.nanocenter.umd.edu/equipment/fablab/sops/etch-07/Oxford%20Chlorine%20Etcher%20SOP.pdf

4.1.1) Log in RIE ICP machine.

4.1.2) Load a blank 4-inch silicon wafer. Run the clean recipe for 10 min.

4.1.3) Take the blank silicon wafer out.

4.1.4) Mount the sample on another clean silicon wafer and load it into the machine.

4.1.5) Run the UV resist etching recipe for 2 min (the recipe can be found in Table 1).

4.1.6) Take the sample out. Load a blank 4-inch silicon wafer. Re-run the clean recipe (can be found in Table 1) for 10 min.

4.1.7) Mount the sample on a clean silicon wafer and load it into the machine.

4.1.8) Run the PMMA etching recipe (can be found in Table 1) for 2 min.

Note: Now the residual resist has been etched and substrate is exposed.

4.2) Cr e-beam evaporation

4.2.1) Log into e-beam evaporator.

4.2.2) Load the Cr metal source and sample into the chamber.

4.2.3) Set the thickness (20 nm) and deposition rate (0.03 nm/sec).

4.2.4) Pump the chamber until required vacuum (10^{-7} Torr) is reached.

4.2.5) Start the deposition process.

4.2.6) Take the sample out after the deposition finishes.

4.3) Cr lift-off procedure

4.3.1) Immerse the sample in acetone with ultrasonic agitation for 5 min.

4.3.2) Clean the sample by rinsing with acetone, methanol and isopropanol.

Note: The Cr evaporated on the resist will be lifted off and a Cr mask for substrate etching is formed.

5. ~~High contrast grating etching~~TiO_2 deposition

~~5~~5.1) Load sample

5.2) Set the parameters for the direct current magnetron sputtering machine

5.1.1) Chamber pressure: 1.5 mTorr, Ar flow: 100 SCCM, Sputtering power: 130 W

5.1.2) Temperature: 27 °C, Stage rotation speed: 20 rpm

5.3) Start the sputter process and stop at desired thickness

5.4) Take the sample out and anneal the TiO_2 film in oxygen environment at 300 °C for 3 hr.

6. High contrast grating etching

6.1) Log in the inductively coupled plasma (ICP) reactive ion etching (RIE) machine.

~~5~~6.2) TiO_2 etching

~~5~~6.2.1) Load a blank 4-inch silicon wafer.

~~5~~6.2.2) Start and run the clean recipe (can be found in Table 1) for 10 min.

~~5~~6.2.3) Unload load the blank wafer and load the sample with Cr mask.

~~5~~6.2.4) Set etching time. Start TiO_2 etching recipe. The etching process will automatically stop.

~~5~~6.2.6) Unload the sample.

~~5~~6.3) SiO_2 etching

~~5~~6.3.1) Repeat the step 5.2 except use the SiO_2 etching recipe.

~~6~~7. Reflectance measurement

~~6~~7.1) Log in and turn on the measurement system.

~~6~~7.2) Place the reflectance standard mirror on the sample holder and align the optical path.

~~6~~7.3) Calibrate the system for the 100% reflectance.

~~6~~7.4) Take off the reflectance standard mirror and place the HCG.

~~6~~7.5) Measure the reflectance of the HCG.

~~6~~7.6) Save the data and log out of the measurement system.

REPRESENTATIVE RESULTS:

Figure 1 shows the implementation of the dispersive element (multilayer high contrast grating (HCG)) in a concentrated photovoltaic system. The sun light is first reflected by the primary mirror and impinges on the reflective dispersive element, where the beam is reflected and split into different bands of different wavelengths. Each band will impinge on a certain location on the solar cell array for the best absorption and conversion to electricity. The key to this system is the design and implementation of the dispersive element, which is composed of multiple layers of HCG.

Figure 2 shows the numerical optimization result for each layer in the dispersive element. ~~The results was calculated by the finite-difference time-domain (FDTD)[7] based commercial simulation software "Lumerical" and further validated by rigorous coupled-wave analysis (RCWA)[8]. The refractive index of TiO_2 was from the SOPRA[9] online database. The optimized six-layer dispersive element can provide a total reflection of more than 90% over the entire solar spectrum.[10,11]~~The results was calculated by the finite-difference time-domain (FDTD)[7] based commercial simulation software "Lumerical" and further validated by rigorous coupled-wave analysis (RCWA)[8]. The refractive index of TiO_2 was from the SOPRA[9] online database. The optimized six-layer dispersive element can provide a total reflection of more than 90% over the entire solar spectrum.[10,11]

To demonstrate the broadband reflectance of HCG experimentally, one of the six layers in the dispersive element HCG structure is fabricated using nanoimprint fabrication. As shown in Figure 3, each grating block consists of two parts. The material of the top grating is TiO_2 and the material of the sub grating is fused silica. The pitch of the 2D HCG is 453 nm. The line width of each grating is 220 nm. The height of both top and sub grating is 340 nm. The material of the substrate is the same as the sub grating.

TiO_2 was deposited on fused silica at HP Labs using a direct current magnetron sputter machine. The chamber pressure was 1.5 mTorr with an Ar flow about 100 sccm. The sputter power was 130 W and the rate was 4 nm/min. Two batches of TiO_2 film were sputtered at different temperatures, 27 °C and 270 °C respectively. To ensure an even film deposition, substrate stage rotation was turned on (20 rpm) during sputtering. Both batches of TiO_2 films were annealed at 300 °C for 3 hours after sputtering to improve film quality. After deposition, both batches of TiO_2 films were examined using a scanning electron microscope (SEM) (Figure 4). The refractive indices of TiO_2 films were also measured (Figure 5). The measured refractive indices were 10% lower than standard database, because the film was porous which can also be observed in Figure 4. A higher sputtering temperature could increase the refractive index, however the roughness of the film was much higher. To reach a good balance between refractive indices and film roughness, the TiO_2 film which was sputtered at 27 °C was chosen as the grating material.

The major steps for nanoimprint fabrication are schematically shown in Figure 6. First, a mold with certain patterns is pressed onto the UV-curable resist on the substrate. Then UV light is applied to cure the resist. After curing, the mold can be separated from the substrate and the shape of resist is exactly the opposite of the mold. The imprinted pattern can be used as the mask to etch the residual resist, deposit metal, lift off and finally etch into the substrate. In this way, the shape of the mold gets transferred into the substrate.

~~To fabricate 2D HCG, a mold is duplicated from a 1D periodic grating silicon master which was fabricated by interference lithography[12]. Then the same mold is used to imprint twice in orthogonal directions on the same silicon substrate to pattern a 2D hole array (Figure 7). The hybrid nanoimprint[13] process can make large-area samples with high-resolution and little defects. The imprinted results (2D hole array silicon array) is shown in Figure 8.~~
To fabricate 2D HCG, a mold is duplicated from a 1D periodic grating silicon master which was fabricated by interference lithography[12]. Then the same mold is used to imprint twice in orthogonal directions on the same silicon substrate to pattern a 2D hole array (Figure 7). The hybrid nanoimprint[13] process can make large-area samples with high-resolution and little defects. The imprinted results (2D hole array silicon array) is shown in Figure 8. The roughness of edges can be further reduced with the help of edge smoothing technologies[14].

After nanoimprint patterning and Cr mask array is completed, an ICP RIE machine is used to etch the sample. Two different etching recipes were developed for TiO_2 and fused silica respectively, which is shown in table 1. The fabricated structure is shown in Figure 9.

The reflectance (from the normal incidence) of 2D HCG was measured using two different spectrometers with different types of detectors, the normal detector and the sphere integration detector. In contrast to sphere integration detector, the normal detector has a relatively small angle of acceptance and therefore will not receive the scattered light. As shown in Figure 10, the difference in reflectance curves measured by both detectors indicates that the light is scattered by the HCG due to the structure roughness. The difference between integration sphere measurement and simulation data is mainly due to the loss of material and fabrication errors. The reflectance curves can demonstrate that the fabricated device can work as a band reflector as one layer in the dispersive element. Due to the high contrast of index between the grating and the substrate, HCG has good angle independence. The reflectance curve will not change much when the incidence angle is less than 15°.

Figure 1: The implementation of the dispersive element (multiplayer HCG) in a concentrated photovoltaic (CPV) system

Figure 2: Numerically optimized reflectance curves for the dispersive element design (six-layer stacked HCG) that can cover most of the solar spectrum

Figure 3: The optimized structure of a HCG for demonstration of nanoimprint fabrication

Figure 4: The SEM images (cross-sectional view) of sputtered TiO_2 films at (a) 27 °C and (b) 270 °C

Figure 5: Measured and standard refractive (SOPRA database) indices of sputtered TiO_2 films

Figure 6: Nanoimprint fabrication process

Figure 7: The SEM image of 2D hole array silicon master (top-down view)

Figure 8: The photo of 2D hole array silicon master fabricated by PDMS-based nanoimprint

Figure 9: The SEM image (cross-sectional view) of the fabricated 2D HCG

Figure 10: One simulated reflectance curve and two measured reflectance curves using sphere integration detector and normal detector respectively

Figure 11: (a) Effect of refractive index on HCG reflectance; (b) Effect of sidewall angle on HCG reflectance

Table 1: The table of etching recipes for TiO_2, fused silica, UV resist, PMMA and clean.

DISCUSSION:

First, the quality of the TiO_2 film is very crucial for the HCG performance. The reflectance peak will be higher if the TiO_2 film has less loss and surface roughness. The TiO_2 film with a higher refractive index is also favorable because the optical mode confinement will be enhanced by a higher contrast in index, which can give rise to a flatter and broader reflectance band in HCG.

Second, the fabrication errors will have significant effects on the HCG and should be avoided. The roughness introduced in fabrication will cause more light to be scattered, so the reflectance will become lower. The deviation of parameters in HCG fabrication including line width, height and pitch will not allow the device to work optimally as in simulation. Moreover, the reflectance of HCG strongly depends on the etching profile, i.e. the angle of sidewall. In Figure 11, the effect of sidewall angles on the reflectance of HCG is numerically calculated. As the sidewall angles decrease from 90° to 84°, the average reflectance drops from over 90% to less than 50%, because the HCG behaves more like a cone-shaped anti-reflection coating when the sidewall angle is small.

The optical efficiency of the dispersive element is important for the overall efficiency of the CPV system, so the reflectance of each layer of HCG should be as high as possible. Based on the discussion above, while the optical efficiency for the fabricated layer is about 60%, there are several possible improvements for a better HCG reflectance. The TiO_2 sputtering condition can be further optimized to generate the film with a higher index, less surface roughness and lower optical loss. The dry etching recipes should be further adjusted for a better etching profile, making the grating straighter, which can be achieved by adjusting the combination of gases (C_4F_8, $SF_6$and O_2) to balance the etching and re-deposition process. The nanoimprint and lift-off process should be improved to avoid roughness and fabrication errors so that the unnecessary scattering can be reduced to increase the overall optical efficiency.

By stacking multiple layers of two-dimensional HCGs with different pitches, the dispersive mirror can operate in much broader spectrum. The mirror can reflectively direct light into different angles according to wavelengths, in a way of packaging all HCG layers subsequently in different tilting angles. Moreover, the dispersive mirror can be fabricated using nanoimprint lithography (NIL) in a large area and at a low cost. Moreover, the proposed system features an easy integration with existing concentrator photovoltaic (CPV) setup so it has the potential to be accepted widely by the industry to improve solar energy conversion efficiency.

DISCLOSURES:

The authors have nothing to disclose.

ACKNOWLEDGMENTS:

This research was supported as part of the Center for Energy Nanoscience, an Energy Frontier Research Center funded by the U.S. Department of Energy, Office of Science under Award Number DE-SC0001013. We also want to thank Dr. Max Zhang and Dr. Jianhua Yang of HP Labs for their help on TiO_2 film sputtering and refractive indices measurement.

REFERENCES:

~~1 Horne, S. *et al.* A Solid 500 Sun Compound Concentrator PV Design. *Photovoltaic Energy Conversion, Conference Record of the 2006 IEEE 4th World Conference on.* 694-697, doi: 10.1109/WCPEC.2006.279550(2006) .~~

~~2 Guter, W. *et al.* Current-matched triple-junction solar cell reaching 41.1% conversion efficiency under concentrated sunlight. *Applied Physics Letters* **94**, 223504 , doi: 10.1063/1.3148341(2009).~~

~~3 Shockley, W. & Queisser, H. J. Detailed Balance Limit of Efficiency of p-n Junction Solar Cells. *Journal of Applied Physics* **32**, 510-519, doi: 10.1063/1.1736034 (1961).~~

~~4 Green, M. A. Potential for low dimensional structures in photovoltaics. *Materials Science and Engineering: B* **74**, 118-124, doi: 10.1016/S0921-5107(99)00546-2 (2000).~~

~~5 Karagodsky, V. & Chang-Hasnain, C. J. Physics of near-wavelength high contrast gratings. *Opt. Express* **20**, 10888-10895, doi: 10.1364/OE.20.010888(2012).~~

~~6 Chou, S. Y., Krauss, P. R. & Renstrom, P. J. Nanoimprint lithography. *Journal of Vacuum Science & Technology B: Microelectronics and Nanometer Structures* **14**, 4129-4133, doi:10.1116/1.588605 (1996).~~

~~7 Namiki, T. A new FDTD algorithm based on alternating-direction implicit method. *Microwave Theory and Techniques, IEEE Transactions on* **47**, 2003-2007, doi: 10.1109/22.795075 (1999).~~

~~8 Moharam, M. G. & Gaylord, T. K. Rigorous coupled-wave analysis of planar-grating diffraction. *J. Opt. Soc. Am.* **71**, 811-818, doi: 10.1364/josa.71.000811 (1981).~~

~~9 Smilab, S. nk Database. *World Wide Web: http://www.sopra-sa.com*.~~

~~10 Yao, Y., Liu, H. & Wu, W. Spectrum splitting using multi-layer dielectric meta-surfaces for efficient solar energy harvesting. *Appl. Phys. A* **115**, 713-719, doi: 10.1007/s00339-014-8419-y (2014).~~

~~11 Yao, Y., Liu, H. & Wu, W. Fabrication of high-contrast gratings for a parallel spectrum splitting dispersive element in a concentrated photovoltaic system. *Journal of Vacuum Science & Technology B* **32**, 06FG04-06FG04-6, doi: 10.1116/1.4898198 (2014).~~

~~12 Solak, H. H. *et al.* Sub-50 nm period patterns with EUV interference lithography. *Microelectronic Engineering* **67**, 56-62, doi: 10.1016/S0167-9317(03)00059-5 (2003).~~

~~13 Li, Z. *et al.* Hybrid nanoimprint− soft lithography with sub-15 nm resolution. *Nano letters* **9**, 2306-2310, doi: 10.1021/nl9004892 (2009).~~

1 Horne, S. *et al.* A Solid 500 Sun Compound Concentrator PV Design. *Photovoltaic Energy Conversion, Conference Record of the 2006 IEEE 4th World Conference on.* 694-697, doi: 10.1109/WCPEC.2006.279550(2006) .

2 Guter, W. *et al.* Current-matched triple-junction solar cell reaching 41.1% conversion efficiency under concentrated sunlight. *Applied Physics Letters* **94**, 223504 , doi: 10.1063/1.3148341(2009).

3 Shockley, W. & Queisser, H. J. Detailed Balance Limit of Efficiency of p-n Junction Solar Cells. *Journal of Applied Physics* **32**, 510-519, doi: 10.1063/1.1736034 (1961).

4 Green, M. A. Potential for low dimensional structures in photovoltaics. *Materials Science and Engineering: B* **74**, 118-124, doi: 10.1016/S0921-5107(99)00546-2 (2000).

5 Karagodsky, V. & Chang-Hasnain, C. J. Physics of near-wavelength high contrast gratings. *Opt. Express* **20**, 10888-10895, doi: 10.1364/OE.20.010888(2012).

6 Chou, S. Y., Krauss, P. R. & Renstrom, P. J. Nanoimprint lithography. *Journal of Vacuum Science & Technology B: Microelectronics and Nanometer Structures* **14**, 4129-4133, doi:10.1116/1.588605 (1996).

7 Namiki, T. A new FDTD algorithm based on alternating-direction implicit method. *Microwave Theory and Techniques, IEEE Transactions on* **47**, 2003-2007, doi: 10.1109/22.795075 (1999).

8 Moharam, M. G. & Gaylord, T. K. Rigorous coupled-wave analysis of planar-grating diffraction. *J. Opt. Soc. Am.* **71**, 811-818, doi: 10.1364/josa.71.000811 (1981).

9 Smilab, S. nk Database. *World Wide Web: http://www.sopra-sa.com*.

10 Yao, Y., Liu, H. & Wu, W. Spectrum splitting using multi-layer dielectric meta-surfaces for efficient solar energy harvesting. *Appl. Phys. A* **115**, 713-719, doi: 10.1007/s00339-014-8419-y (2014).

11 Yao, Y., Liu, H. & Wu, W. Fabrication of high-contrast gratings for a parallel spectrum splitting dispersive element in a concentrated photovoltaic system. *Journal of Vacuum Science & Technology B* **32**, 06FG04-06FG04-6, doi: 10.1116/1.4898198 (2014).

12 Solak, H. H. *et al.* Sub-50 nm period patterns with EUV interference lithography. *Microelectronic Engineering* **67**, 56-62, doi: 10.1016/S0167-9317(03)00059-5 (2003).

13 Li, Z. *et al.* Hybrid nanoimprint− soft lithography with sub-15 nm resolution. *Nano letters* **9**, 2306-2310, doi: 10.1021/nl9004892 (2009).

14 Yu, Z., Chen, L., Wu, W., Ge, H. & Chou, S. Y. Fabrication of nanoscale gratings with

reduced line edge roughness using nanoimprint lithography. *Journal of Vacuum Science & Technology B* **21**, 2089-2092, doi: 10.1116/1.1609471 (2003).